STUDY AIR FLOW DISTRIBUTION IN THE DRYER SYSTEM THROUGH CFD SIMULATION

ABDULRAHMAN TAHER AHMED ANAAM

UNIVERSITI TEKNIKAL MALAYSIA MELAKA

STUDY AIR FLOW DISTRIBUTION IN THE DRYER SYSTEM THROUGH CFD SIMULATION

ABDULRAHMAN TAHER AHMED ANAAM

This report is submitted
in fulfillment of the requirement for the degree of
Bachelor of Mechanical Engineering (Thermal and Fluids)

Faculty of Mechanical Engineering

UNIVERSITI TEKNIKAL MALAYSIA MELAKA

MAY 2017

DECLARATION

I declare that this project report entitled "Study Air Flow Distribution In The Dryer System Through CFD Simulation" is the result of my own work except as cited in the references

Signature : ....

Name : ....

Date : ....

APPROVAL

I hereby declare that I have read this project report and in my opinion this report is sufficient in terms of scope and quality for the award of the degree of Bachelor of Mechanical Engineering (Thermal & Fluids).

Signature	:	....
Name of Supervisor	:	....
Date	:	....

DEDICATION

I dedicate this report my lovely wife, Siti Aisyah Binte Mohammad Ghazali who has constantly given me her endless support, my family and friends, whom without their endless support, I wouldn't be able to continue perusing my higher education. Special thanks and admiration to my supervisor, Dr. Suhaimi Bin Misha for without his wise suggestions, continuous guidance, and direct assistance, this report nor the project, could have gotten off the ground. I would like to thank my university, UTeM and my friends for their support and advice for this internship training. Thank you all for your enduring patience and continuous encouragement.

ABSTRACT

Tray dryer systems are continuously improving to be more efficient. The aim of this project is to increase the drying rate by studying the air flow distribution in the drying chamber using CFD simulation. This is done by re-designing the drying chamber and its trays. The study is being done using Computational Fluid Dynamics in Ansys Fluent. By using this software, it was possible to predict the air velocity and air temperature that flows on top of the trays and throughout the drying chamber. Drying rate is dependent on many factors. Air velocity, air flow distribution, and temperature are the main contributors in determining the drying rate. Four designs were suggested to improve the air distribution on the trays. Average velocity of each tray and the drying chamber, as well as the gap between the maximum and minimum tray average velocity had determined the best air flow distribution design. It was clear that the up-staging design had the most minimum gap as well as the maximum average velocity.

ACKNOWLEDGEMENT

I would like to express my deepest appreciation to my supervisor Dr. Suhaimi Bin Misha for giving me the opportunity to do my final year project with him. He never hesitated to give me advice and guidance whenever I confronted problems. I am thankful for his patience and advice while leading me in this project. I would like to thank my family for their efforts in helping me to complete the final year project and to my friends for their endless support and encouragement. Last but not least, I would like to thank my course mates for giving me their support, patience and encouragement.

CONTENT

LIST OF FIGURES

LIST OF TABLES

CHAPTER 1

INTRODUCTION

1.1 Background

Drying process is one of the most important methods to preserve the agricultural materials such as food, wood, rubber, etc. It is a method that has been used along the lifetime of the homoserines. Drying process is method where it includes dehydration that involves the simultaneously application of heat and removal of moisture from crops or foods so that it's easier to be preserved, stored, and marketed. Heat transfer involves in moving the heat from the heating medium to the point at which evaporation occurs. Once the moisture has been evaporated, the vapors produced must be transported through the product structure to the surrounding medium. This process involves air flow through the structure during the dehydration process. Many factors can cause food spoilage and these factors cannot occur without the moisture (Misha .S, 2013).

One of the traditional ways of drying is spreading the agricultural materials on a wide space where it will be exposed directly to the sunlight. This method of drying these materials is very difficult to control. As well as there are many factors for these materials to take a longer time than it supposed to be and these materials might not be able to be used anymore because of wind, birds, animals, require a large space, etc.

One of the new methods of drying is solar dryer. The air gets heated by the solar collector. Then the heated air flows to the drying chamber. There is a lot of real applications of the solar drying systems, but one of the new concepts design in Malaysia and was introduced (Misha .S, 2013). In his study (Misha .S 2013) introduced and created a new model of solar drying system as shown in Figure 1.1. Where the solar collectors increase temperature

Figure1.1: Drying system. (Misha .S, 2013)

of the water that flow in the copper tube from the tube tank. The hot water flows to heat the air for drying goes to the heat exchanger Figure 1.2. The drying chamber is the area where the trays are located. The required material is placed on top of the trays and spread them to expose them to high temperature airflow, where it passes through the desiccant prior to that. The desiccant is used to extract and reduce humidity from the air flowing to the drying chamber (Misha .S, 2013). However, the details of the hot water generator are not discussed in this project. The scope of this project is to study air flow distribution in the drying chamber through CFD simulator.

Figure 1.2: Drying chamber. (Misha .S, 2013)

1.2 PROBLEM STATEMENT

The tray dryers are the most broadly utilized due to its basic and cheap design as in Figure 1.3. The required material to be dried is spread out on these trays. the tray dryer can dry more items as well as these materials can be stacked as the trays are orchestrated at various levels. Most tray dryers utilize hot air stream where moisture is vaporized from the materials and extracted from airflow. To produce the uniform dehydration is to have uniform air stream, which is distributed equally on each tray. The positions of trays in the in the drying chamber will determine the uniformity of air flow distribution. (Misha .S, 2013) introduced different arrangement of trays to have more distributed uniform air stream. In this Final Year Project, air flow distribution in the dryer system will be studied by changing and manipulating the arrangement of the trays to find if there are any improvements with new arrangement through CFD simulation.

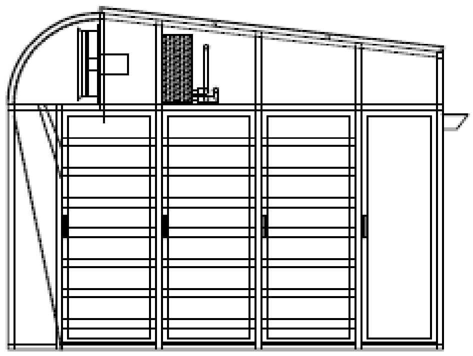

Figure1.3: The drying chamber, and in the middle, is the trays, (Misha .S,2013)

1.3 OBJECTIVE

The objectives of this project are as follows:

1. To modify the existing trays positions in the drying chamber.
2. Investigate the air flow distribution in the drying chamber using Computational Fluid Dynamics (CFD) software.
3. To predict the drying uniformity on each one of the trays,

1.4 SCOPE OF PROJECT

The scopes of this project are:

1. Re-locating or re arranging the trays using ANSYS.
2. A simulation of air stream lines, air distribution, and air velocity on the new re-located trays using ANSYS.
3. Observation of air distribution on the re-arranged tray using ANSYS.
4. Find the average velocity of air above the product.
5. Perfect the drying rate of each tray.

1.5 GENERAL METHODOLOGY

The actions that need to be carried out to achieve the objectives in this project are listed:

1. Literature review:

   Journals, articles, or any materials regarding the project will be reviewed.

2. Design:

   Develop the model. Sketch the new trays with specific dimension, choosing the new location.

3. Running Simulation:

   Visualization of simulation of air distribution.

4. Analysis and comparing:

   Analysis will be carried out on how hot air is distributed on the trays for all the different designs that will be presented. Comparing the results of each design to each other and suggest the best design based on the results presented.

5. Report writing:

   A report on this study will be written at the end of the research.

The methodology of this study is summarized in the flow chart as shown in Figure 1.4.

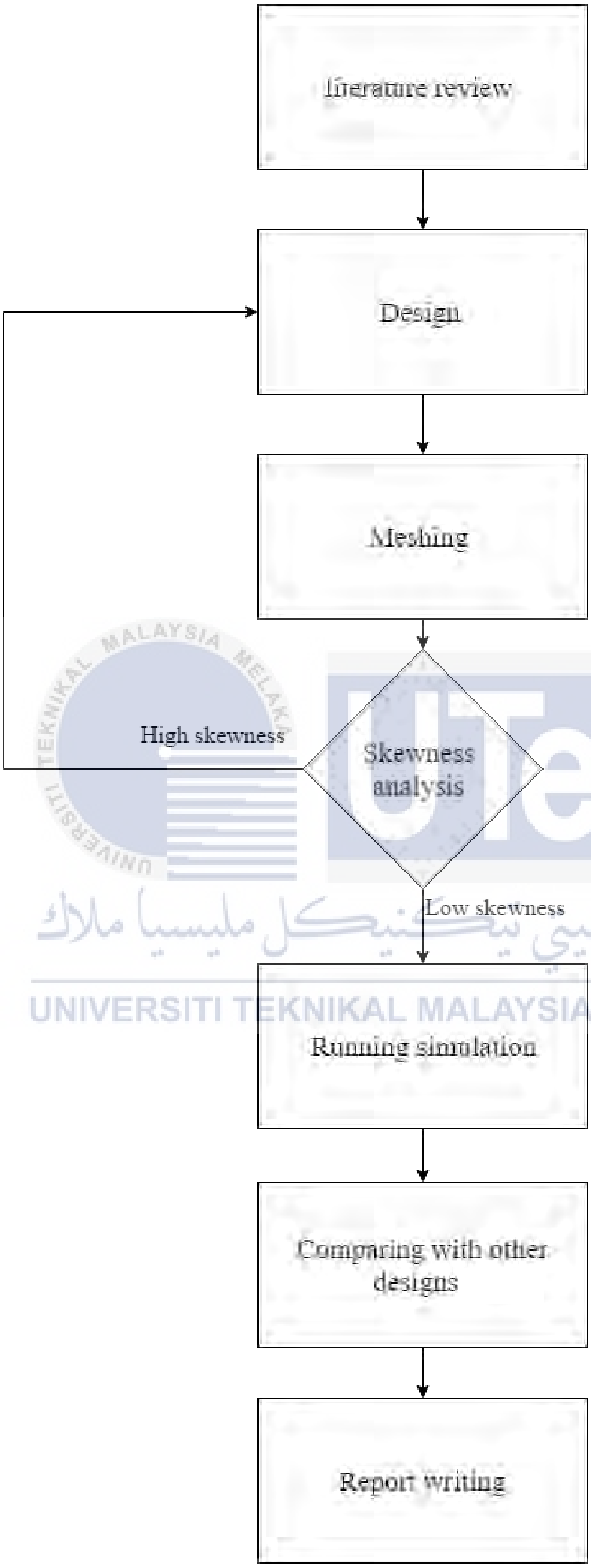

Figure 1.4: Methodology flow chart

CHAPTER 2

LITERATURE REVIEW

In this chapter, the most important journals will be reviewed as well as some will be referenced. This is done to have a clearer image about the future of this project and to have a better understanding of the theories.

2.1 Computational Fluid Dynamics

It can be very dangerous, expensive, time consuming and difficult for most of the experiments to run in order to find the results for the specific parameters, especially putting in consideration the error percentage for a large scale solar drying chamber and its trays as well as repositioning them to get the results (Misha .S, 2013). Computational fluid dynamics (CFD) simulation is widely used because of its ability to solve complicated equations for the conservation of momentum, energy, and mass using numerical methods to find and predict each of the pressure profiles, velocity, temperature at any point or any position needed in the drying chamber. Computational fluid dynamics (CFD) is used in this project to simulate the velocity and temperature profiles at each tray in the drying chamber, as well as the fluid pressure if required (Misha .S, 2013).

The CFD is utilized as an instrument to predict the temperature in the drying chamber as well as the air flow distribution to acquire the uniform drying. CFD has additionally been widely utilized as a part of food industry to explore the stream example of the air in the drying chamber. Uniform airflow distribution in the drying chamber is important in light of the fact that it gave huge impact on the proficiency and the homogeneity of the items being dried (Misha .S, 2013).

2.2 Designs of the drying chamber

The design of the drying chamber is very important due to its capability to affect the airflow distribution. Designing and locating the trays as well as placing them in a pattern is just as important as the design of the drying chamber itself. This is because placing the trays at the exact proper position, and having them positioned in the proper pattern can help reduce the drying time and drying uniformity at each tray. Normally, trays that are far from the source will take longer time to get dried.

Drying is the process of mass transfer and heat to remove the water or any other solvent by evaporation from a liquid, solid, or semi-solid. Typically, hot air stream is applied to dry any material, and usually the drying process is separated into two phases. In the first phase, the surface and inner side of the item have the same dampness content at first. The surface of the product or the material will be saturated with vapour when it gets heated by hot air, and then the water will evaporate. In the second phase, when the material surface gets dried, the moisture will slowly move from the inner side of the material to the outer surface, having it exposed to the dry airflow and high temperature to evaporate that moisture. Be that as it may, a few materials do not go through neither of the first or second phases. Belessiotis and Delyannis (2011) are characterized under another phase. On the third phase, for hygroscopic materials where the dampness content keeps on evaporating until the material accomplish its equilibrium stage. However, most materials quit drying before this phase.

Drying time relies on the way the material behaves in nature and the drying conditions. Imperative parameters in the drying procedure are mugginess, temperature, and wind stream rate. A few materials like food, and other materials that are sensitive to heat are not appropriate for drying at high temperature since material quality might be debased or harmed. Drying utilizing desiccant material produces dry air since the desiccant material adsorbs dampness from the air. The handled air delivered after dehumidification is dry, as well as increments in temperature because of the isothermal process. Drying at low temperature and dampness can only be completed utilizing a desiccant, which can keep up the colours of the material which in this case its food. Other drying strategies can just create low humidity in the air at high temperatures.

Utilizing an alternate drying process, a similar item demonstrated critical impacts in surface, shading, and supplement content (Misha .S, 2012)

The hybrid solar thermal drying system in the present work was developed from a mixed mode common convection solar dryer, regular convection thermal back up unit, and recuperation dryer (Tadahmun A. Yassen, 2016). The mixed mode regular convection solar crop-dryer is possibly best and it seems, by all accounts, to be especially encouraging in tropical moist zones where climatic conditions support sun drying of agrarian items. The regular convection sun powered dryer was built from single pass twofold stream sun based air radiator with the roughened safeguard plate and drying chamber. The recuperation dryer was a half breed dryer built from an immediate sort regular convection sunlight based dryer and rectangular conduit. The warm go down unit involves gas-to-gas warm exchanger and fuel burner. (Tadahmun A. Yassen, 2016)

The drying chamber was made from aluminum angles to prevent heavy weight. The drying chamber size is (1100 mm in width × 420 mm in depth × 900 mm in height). The dryer connected with the solar collector directly through the duct the trays are made portable to permit loading, unloading and cleaning. The trays were placed on top of each other in order of bottom tray, middle tray, and top tray or as shown in Figure 2.1.

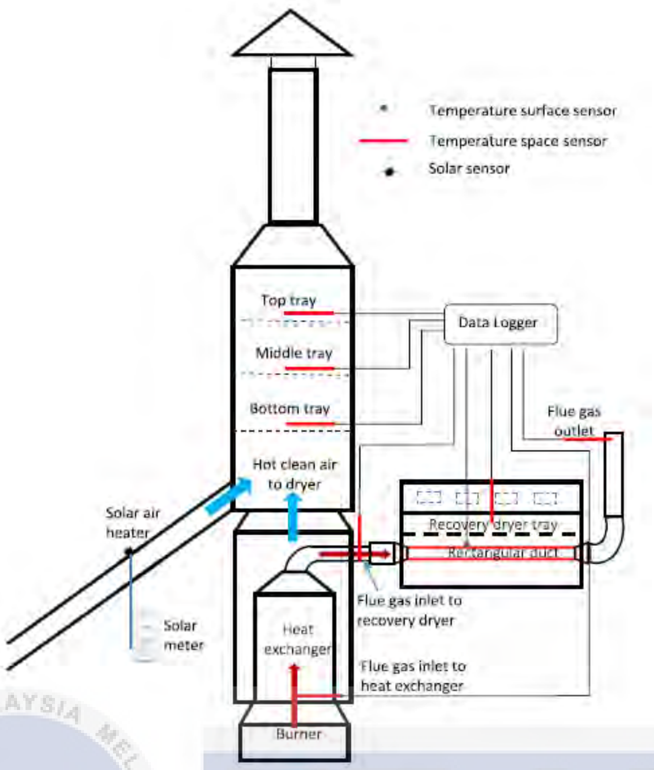

Figure 2.1: Hybrid solar thermal drying system. Source: (Tadahmun A. Yassen, 2016)

The hybrid solar thermal drying system have the trays placed on top of each other leaving a gap between each tray and the one above it. This pattern creates a various drying rate for each of the trays. So, the bottom tray gets heated first which allows the material placed on that tray to get dried first. Time delay will occur in drying each of the rest of the trays, because the bottom tray gets the most of heat as well as the airflow. After that, the middle tray gets dried and the top tray will be the last to get dried. This non-uniform drying rate can affect the quality of the material that is required to get dried, in which the bottom tray gets dried first. During the top and middle still in the process of drying their material, the bottom tray would have its full drying period. By the time the rest of the trays have completed their drying time the bottom tray will be a little over dried, which can affect the quality of the material. The same issue happens between the middle and the top tray (Tadahmun A. Yassen, 2016). The Figure 2.2 this affect by looking at the temperature difference in the early stages. the hybrid solar thermal drying system cannot contain big amounts of materials due its number of trays in the drying chamber.

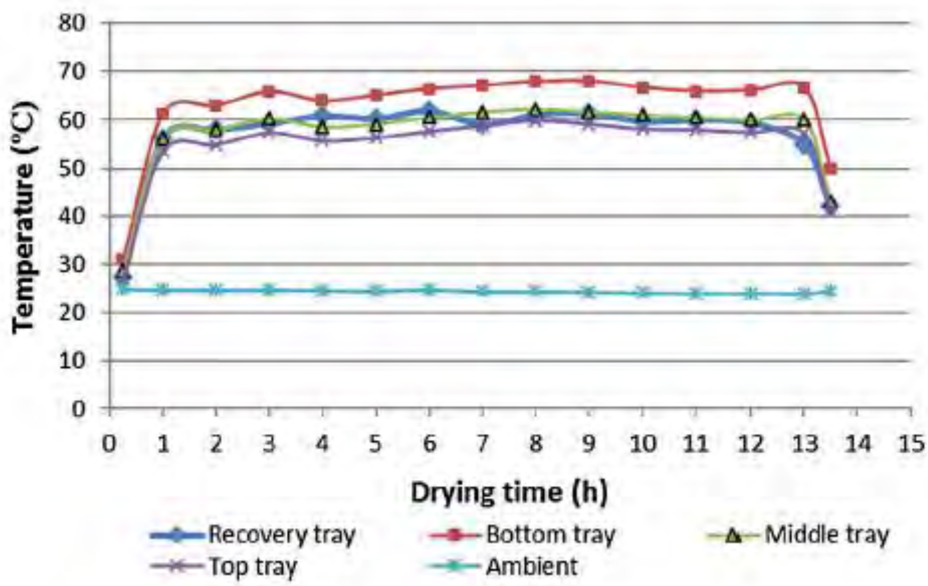

Figure2.2: Variations in the tray and ambient temperatures with drying time. Source (Tadahmun A. Yassen, 2016)

In conclusion, the hybrid solar-thermal dryer was combined with supplementary recuperation dryer has been explored tentatively. The present hybrid solar-thermal dryer system was improved by using from the heat waste through the vent gasses outlet from the thermal back-up unit by utilizing the recuperation dryer or recovery dryer. The correlation between the mixture dryer with and without recuperation dryer was finished. It is obvious from the outcomes and the performance assessment of this system experiment that the improvement was meant to be in the recovery dryer.

The new design of drying system in this research was made for drying osmotically dehydrated cherry tomatoes (Nabnean .S, 2016). This drying system consist of heat exchanger, drying chamber, water type heat storage unit, and water type solar collector. The drying chamber size is 3 m long × 1 m wide × 1.4 m high, and its maximum capacity is 100kg of osmotically dehydrated cherry tomatoes. The experiment was done by drying three batches of 100-kg of osmotically dehydrated cherry tomatoes.

The process layout of this drying system is shown in Figure 2.3, where the solar collector gets heated by the solar radiation to heat the water flowing through the solar collector. The water goes to the tank and then gets pumped to the heat exchanger to heat the air that received by the inlet. The air gets pushed to the trays by the blower or fan to enable the drying process to continue. The water is cooled down after the simple heat transfer process which it is convection in this system as shown in Figure 2.4. Then the water goes back to the tank to be stored and pumped to the solar collector to start the process all over again.

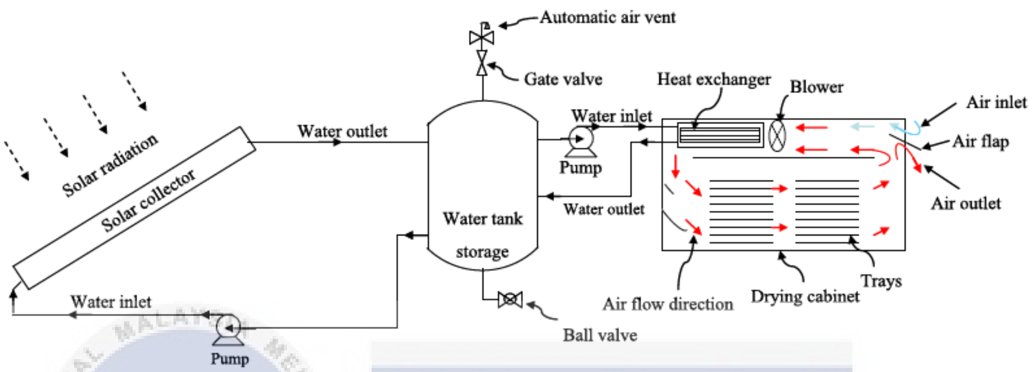

Figure 2.3: The process layout, source (Nabnean .S, 2016).

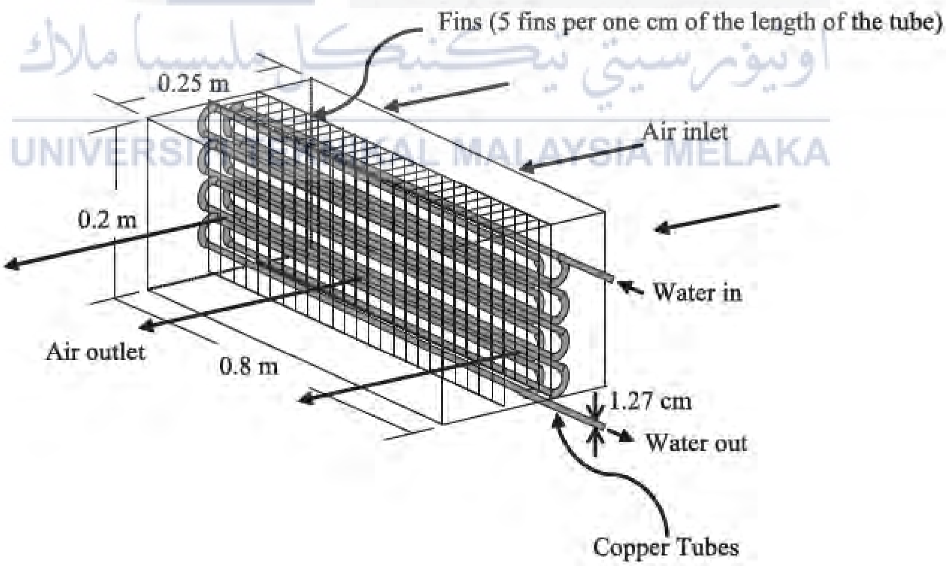

Figure2.4: Diagram of the heat exchanger, source (Nabnean .S, 2016).

The drying chamber is 3 m long × 1 m wide × 1.4 m high, and has 18 trays which are mounted inside the drying chamber or drying cabinet as in Figure 2.5. Outside air enters by the air inlet channel into the heat exchanger, and the heated air leaves the heat exchanger. At that point, the heated air from the heat exchanger goes to the drying material spread in the thin layers on 18 on horizontal levelled trays that are stacked in two vertical groups of trays in columns. Each tray is made of aluminium casing and aluminium net with the measurement of 0.9 m × 1.0 m. The trays are of sifter sort to permit air flow and circulates through the drying material. This drying chamber is uncommonly designed in a manner that hot air is guided to streams on the 18 on horizontal levelled trays over the item put in the trays.

In conclusion, this design was made to contain 100kg of osmotically dehydrated cherry tomatoes, but to reduce the drying time a spacing need to made between the trays as well as increase the number of trays to carry more materials.

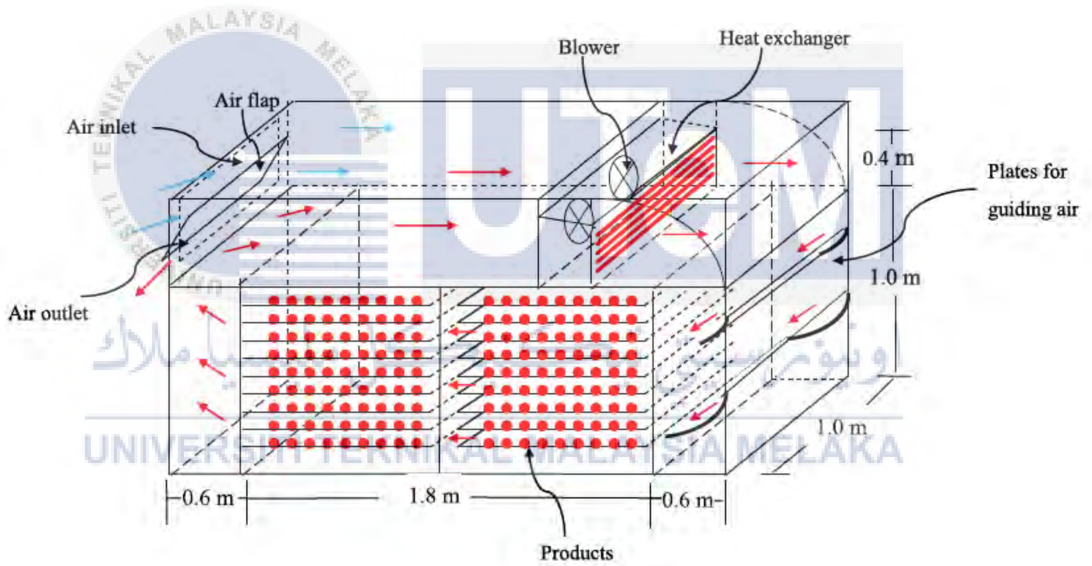

Figure 2.5: Schematic diagram of the drying cabinet, source (Nabnean .S, 2016).

In this study, exergy investigation was conducted for a rotating tray dryer that is equipped with a crossflow plate heat exchanger amid drying of apple cuts (Ghasemkhani .H, 2016). Three drying air temperatures and tray rotation speeds in the scope of 50–80 °C and 0–12 rpm, separately, were utilized. Two drying air speeds in the scope of 1–2 m/s were balanced for each drying temperature and rotation speed with and without use of the heat exchanger. The experiments were done to evaluate the impacts of the test factors on the exergetic execution parameters of the dryer. Additionally, the impact of drying conditions on the nature of dried apple slices was evaluated by deciding apparent density, rehydration ratio, surface color, and shrinkage. (Ghasemkhani .H, 2016).

The rotating tray convective dryer is fitted with an air to air crossflow heat exchanger was planned and created to recuperate waste heat from over flowing air and enhance air dispersion inside the drying chamber Figure. 2.6. The dryer made of a control panel, a heat exchanger, an electrical heater, a drying chamber, a closure, air flow pipes, a DC electric motor, a shaft and two bearings, inverter, and adjustable centrifugal blower. The cylindrical-shaped drying cabinet with 86 cm in diameter and 40 cm in height was fabricated utilizing 1.2 mm thick stainless steel sheet (Ghasemkhani .H, 2016). The conclusion was made on the drying cabinet to remove and place the sample trays amid drying experiments. The system was sealed with a gasket to keep the heat wastage from drying cabinet. The four stainless steel trays are to be measured of 30 × 30 cm were situated inside the drying chamber with an edge of 90° in respect to each other.

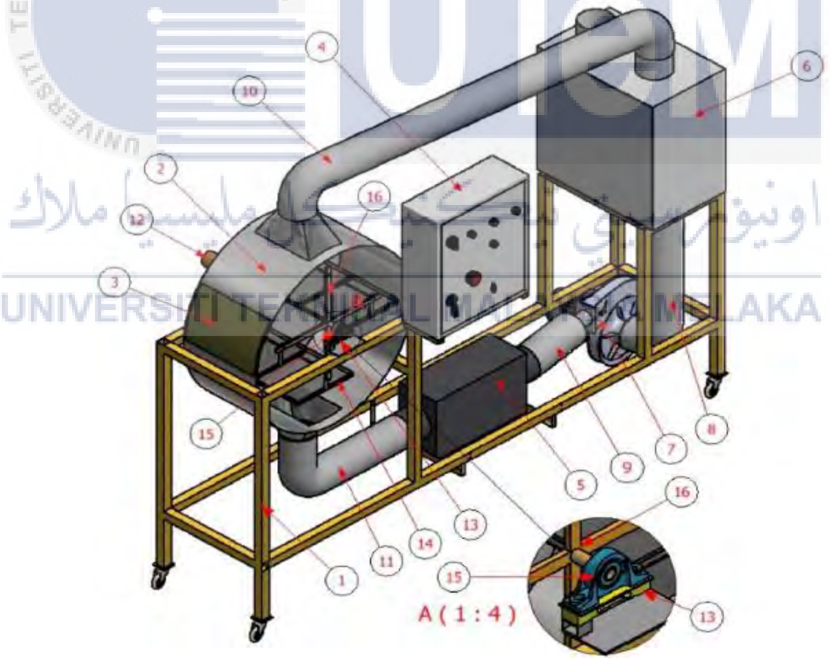

Figure 2.6: Schematic of the dryer. 1, frame; 2, drying chamber; 3, closure; 4, control panel; 5, heater; 6, heat exchanger; 7, blower; 8 and 9, air flow pipes; 10, inflow pipe;11, outflow pipe; 12, DC electric motor; 13, load cell; 14, sample trays; 15, bearing; 16, tray rotation mechanism. Source (Ghasemkhani .H, 2016)

2.3 Drying uniformity in the drying chamber.

Tray dryers are the most generally utilized dryers for different drying applications in view of their low cost and simple design (Misha, 2015). For the most part, a tray dryer comprises of a few piles of trays set in an insulated chamber where hot air is distributed by a normal flow or fan. The uniformity of air stream appropriation over the trays is significant to get uniform item quality. The variety of the last dampness substance of the dried item at various tray late positions is ordinarily experienced as a result of poor airflow distribution.

The experiment drying was done in one days that had an average solar radiation. In the 3-D simulation which was done using CFD was conducted to anticipate the air flow distribution, that's due to the failure of the simulation that was done in 2-D. Since the 2-D simulation wasn't sufficient enough to present the expected results. The velocity was measured by anemometers, where the devices were placed at the end of various trays as shown Figure 2.7. It was done for validation purposes. Unfortunately, the speed was not recorded at all due to the range of the instrument that was between 0.4 m/s and 30 m/s, where the average velocity at all trays were lower than 0.4 m/s which is the minimum velocity that can recorded by the anemometers. However, the velocity of the outlet was recorded to be 8.9 m/s.

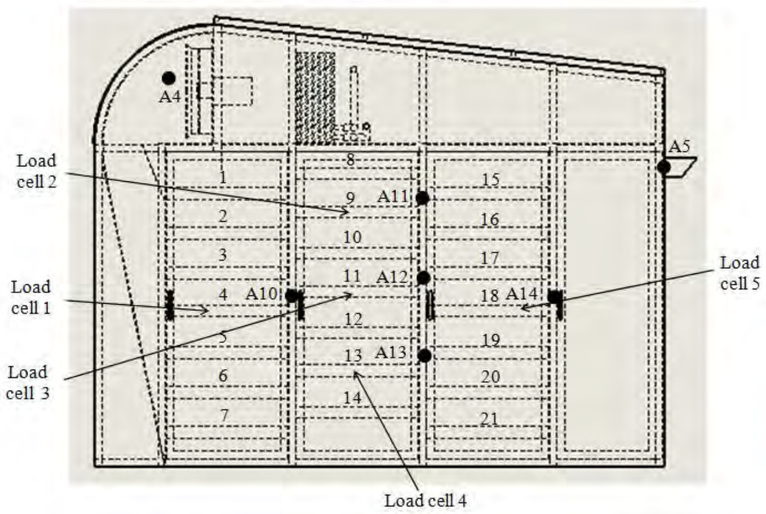

Figure 2.7: Sensors position. (Misha, 2015)

Table 2.1: Velocity of experimental and simulation result. (Misha, 2015)

No.	Anemometer positions	Velocity (m/s)	
		Experiment	Simulation
1	Tray 1	0.8	0.80
2	Tray 2	-	0.15
3	Tray 3	-	0.27
4	Tray 4	0.4	0.41
5	Tray 5	0.6	0.62
6	Tray 6	0.6	0.64
7	Tray 7	0.7	0.73
8	Exit channel	8.9	9.02

The velocity readings were recorded in experiment as well as the simulation results are shown Table 2.1. Both experiment values and the simulation results were tightly close. For tray 2 and tray 3 the velocity wasn't recorded due to the low velocity at both trays. As shown Table 2.1 the percentages of error were very small and validate the simulation.

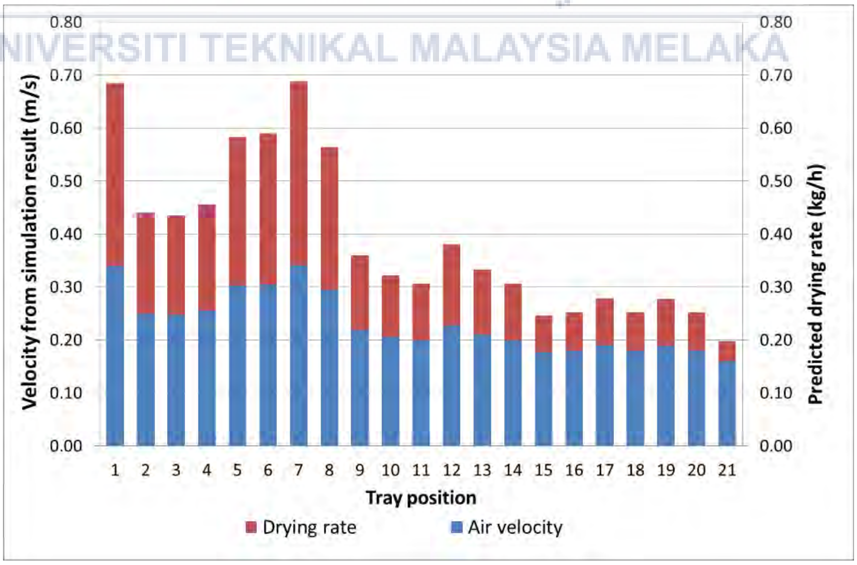

Figure 2.8: Velocity from simulation and predicted drying rate for each tray. (Misha, 2015)

In Figure 2.8, demonstrates the air speed from the simulation and the anticipated drying rate. The result from simulation demonstrates that the most elevated air speed was at tray 1 and 7 and that's extra slope divider and baffle that helped channelling the air to the all top tray level. An experiment was done without the baffle to anticipate and predict air flow distribution in the drying chamber. It was found that without the baffle, the top tray level had less air that was channelled therefore less velocity was at these trays. It can be concluded, based on Figure 2.8, that the air velocity is one of the main contributors and pillars to the drying rate. The higher the velocity that is channelled to the item, the higher drying rate this item will have.

CHAPTER 3

METHODOLOGY

3.1 Introduction

In this chapter, the methodology that is used in this project to create new different designs to help in reaching the objectives mentioned in chapter is being described. The flow chart of the project is shown in Figure 1.4. The project starts by studying the journals that are related to this project, as well as that have the potential to create better understanding and develop the methodology. Next stage is to create the designs that are meant to reach the objectives of this project. The design of drying chamber as shown in Figure 1.2 different arrangement of the tray positions will be done to study the air distribution. On the third stage, is to generate mesh for the designs. Then running the simulation using the same parameters that were proposed (Misha .S, 2013). According to (Misha, 2015) the calculation for the simulation of air flow distribution in the drying chamber have been done. The experiment results show a good agreement with the simulation. Therefore, the simulation will be carried out in this project. Using the same parameters and settings for the simulation, but the agreement of the tray will be changed to study the drying uniformity. On the fourth stage, and after running the simulation, the results will be collected. The last stage, writing the final report will be done. However, a discussion was done with my final year project supervisor that in this semester both literature review and the design will be discussed in this report.

The design of tray positions that will proposed in this project as follows:

1. Up staging trays design.
2. Three column-one level trays design.
3. Two column-one level trays design.
4. Three column-tilted trays design.

3.2 Up-staging trays design

Figure 3.1 shows the up-staging trays design. In which the trays are re-positioned in a same distance from each other in the z axis, but a little bit higher than each other in the y axis. This design was made by the default program of Ansys geometry. The up-staging trays design is proposed due to the expected results that might appear in the simulation. This design may create a path for the air to flow and distribute through the level, and in that way a better air distribution will be established. At the same time the heat and the temperature each tray at the top of each level will increase due to the path that been created by the trays in the level. It is expected that the top front tray will have a higher temperature as well as airflow exposure than the top rear tray. But the top left might have a better airflow and temperature distribution than the third column-one level trays design.

Figure3.1: Up staging trays design (21 tray).

3.3 Three column-one level trays design

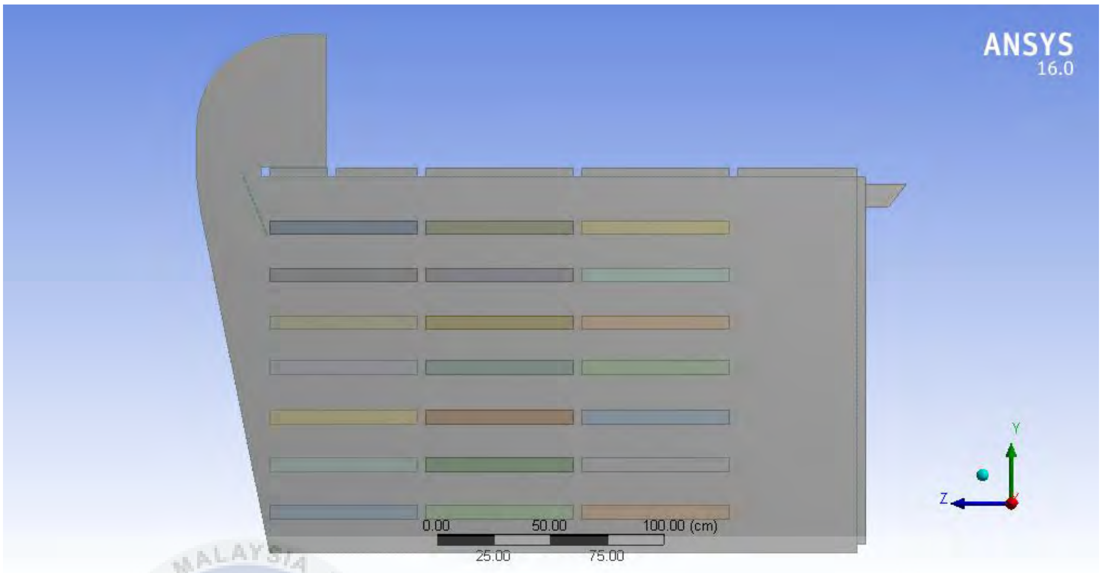

Figure3.2: Three column-one level trays design (21 tray).

The Figure3.2 demonstrates the Three column-one level trays design. Which consist of 21 trays. The trays are positioned in three columns. The top level of trays is connected to a baffle to help channel the air to the level. The three column-one level trays design is proposed to further the studies on the air distribution and drying rate that was done (Misha .S, 2013). Base on the design, it is expected to have a higher drying rate on the surface of the front column trays than rare ones. At the same time the heat and the temperature each tray at the front column trays will be higher due to the design and the re-positioning.

3.4 Two column-one level trays design

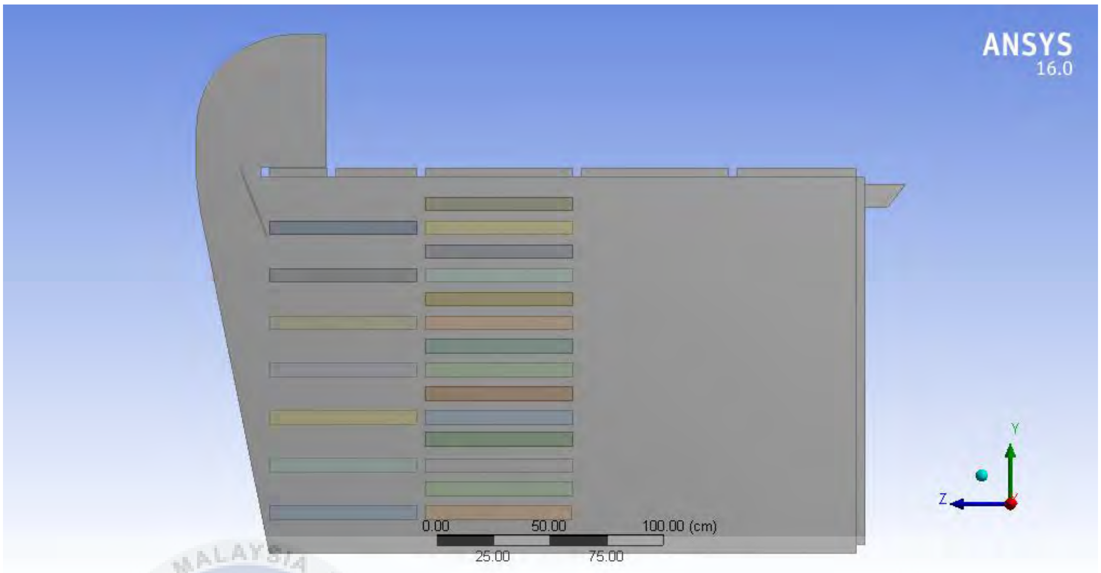

Figure3.3: Two column-one level trays design (21 tray).

The Figure 3.3 demonstrates the two column-one level trays design. Which is maintained to be 21 trays. The trays are re-positioned in to two columns. The top front tray is connected to a baffle. The trays that were at the rare or third column as in (fig3.2) ware shifted to the second column. The two column-one level trays design is proposed due to the study that was done (Misha .S, 2013) that described that the first column has higher drying rate than second, and the second column has a higher than the third column. Therefore, the rare trays were shifted to the second column to have higher drying rate.

3.5 Three column-tilted trays design

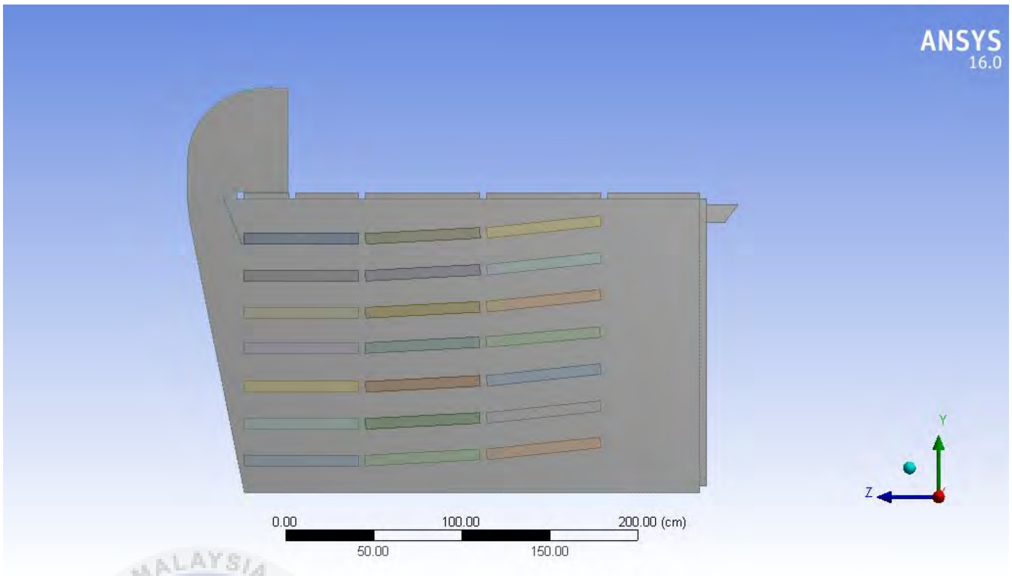

Figure 3.4: Three column-tilted trays design (21 tray).

The Figure 3.4 shows the three column-tilted trays design. Which is also maintained to be 21 trays. The trays are re-positioned to have tilt in the second and the third column. While the font column is maintained to be without any tilt, the second column is tilted with angle of 3°degrees. The third column is tilted with 6° degrees. This tilt is expected to aid with guiding the air flow and expose more surface area which helps with drying the materials quicker.

CHAPTER 4

RESULTS AND ANALYSIS

4.1 MESH

Figure 4.1(a) illustrates the number of nodes and elements that were used in this mesh for three column-one level trays design. It also shows the skewness of the mesh, where it represents the mesh quality. The skewness is a measure of the relative distortion of an element compared to its ideal shape and is scaled from 0 to 1, where 0 is excellent and 1 is unacceptable. The quality of the mesh plays a critical part in the accuracy of the simulation or the numerical computation.

The aspect ratio which is shown in Figure 4.1 (b), is represented in the maximum value. Aspect ratio is a measure of the stretching of the cell. Theoretically, a very large aspect ratio may yield accurate results with fewer cells.

An automatic mesh was used that was created by the default settings of the program, it created an unacceptable skewness as well as high aspect ratio. Therefore, creating a mesh control was necessary for some faces, edges, and bodies. Figure 4.1 (d) shows two body sizing that were used in mesh control for this geometry. Body Sizing was selected to be for 21 trays, while Body Sizing 2 was selected to be for the rest of the geometry. A pinch for several edges was used as a component of this mesh control. Due the small size of the baffle comparing to the rest of the body, a Face Sizing was created by selecting the top and bottom face.

Statistics	
Nodes	107573
Elements	611844
Mesh Metric	Skewness
Min	3.2083e-005
Max	0.90589
Average	0.24018
Standard Devi...	0.12957

(a)

Statistics	
Nodes	107573
Elements	611844
Mesh Metric	Aspect Ratio
Min	1.1602
Max	15.634
Average	1.8851
Standard Deviation	0.50864

(b)

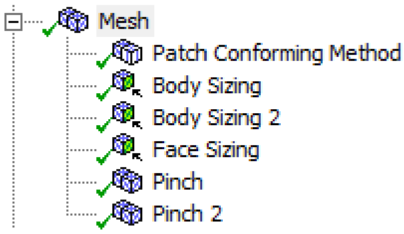

(d)

Figure 4.1: Three column-one level trays design (a) Number of nodes, elements, and the mesh metric of the skewness statistics. (b) Mesh metric of the aspect ratio statistics. (d) Mesh control tree

Figure 4.2 shows the general mesh of up-staging trays design. Where it was possible to generate mesh for this design with in the acceptable range of skewness and aspect ratio which they were found to be 0.9314 and 13.73 respectively as shown in Figure 4.3(a) and (b). This mesh consists of multiple specific mesh, Figure 4.1(d) shows the mesh tree.

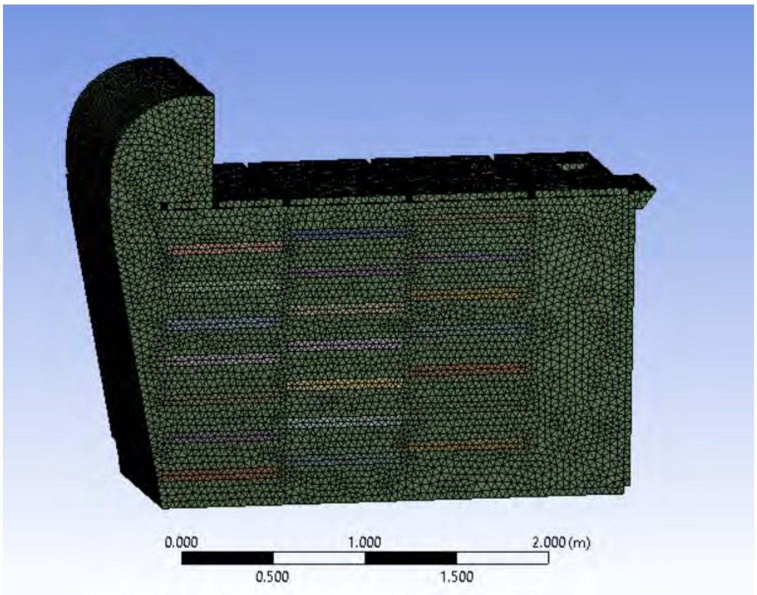

Figure 4.2: General mesh of up-staging trays design.

Much like Three column-one level design, this mesh has two different body sizing. Body sizing is selected to be on the trays with element size of 0.038m, while Body Sizing 2 is selected to be the rest of the body with element size of 0.04m. Face Sizing is selected to be the top and the bottom faces of the buffer with element size of 0.028m. Two pinches were created on one master edge and one salve edge for both pinches. For the general settings, the relevance centre to be coarse, span angle is fine, smoothing to be medium, and the transition to be slow.

Statistics	
Nodes	140729
Elements	794166
Mesh Metric	Aspect Ratio
Min	1.1619
Max	13.73
Average	1.8874
Standard Deviation	0.52043

(a)

Statistics	
Nodes	140729
Elements	794166
Mesh Metric	Skewness
Min	8.7671e-005
Max	0.93135
Average	0.23874
Standard Devi...	0.13132

(b)

Figure 4.3: Up staging trays design (a) Number of nodes, elements, and the mesh metric of the skewness statistics. (b) Mesh metric of the aspect ratio statistics.

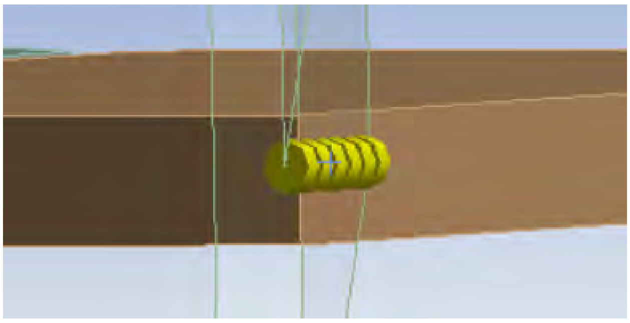

Figure 4.4: Edge sizing 3

For three column-tilted trays design, the mesh control is almost the same as the first two designs. Body Sizing 2 is selected to be similar to previous designs, but the element size is set to be 0.061m. Edge sizing is being added to the mesh control as shown in Figure 4.5 (c). Figure 4.4 shows the selected edge for edge sizing, where the number of divisions is set to be 6 divisions. It is possible with these settings of mesh control to achieve the skewness and the aspect ratio which they were found to be 0.932 and 12.60 respectively as shown in Figure 4.5 (a) and (b).

Nodes	108490
Elements	616875
Mesh Metric	Skewness
Min	2.2226e-004
Max	0.93185
Average	0.24034
Standard Devi...	0.12985

(a)

Nodes	108490
Elements	616875
Mesh Metric	Aspect Ratio
Min	1.1631
Max	12.601
Average	1.8849
Standard Deviation	0.50932

(b)

- Mesh
  - Patch Conforming Method
  - Body Sizing
  - Body Sizing 2
  - Face Sizing
  - Pinch
  - Pinch 2
  - Edge Sizing 3

(c)

Figure 4.5: Three column-tilted trays design (a) Number of nodes, elements, and the mesh metric of the skewness statistics. (b) Aspect ratio statistics (c) Mesh control tree.

For two column-one level trays design, different mesh had to be used in order to get the acceptable range of skewness and aspect ratio. Figure 4.8 (c) shows the mesh control tree that was used. Figure 4.6 (a) show the edge sizing, where the side edges of each tray were selected with the number of divisions to be 25 divisions. While the side top and bottom edges of the trays is selected with 65 number of divisions as shown in Figure 4.6 (b). In edge sizing 3, the bottom front edge is selected with 69 number of divisions as shown in Figure 4.7. The body sizing is being the whole body without 21 trays with element size of 0.046m. Face Sizing is selected to be the bottom of all 21 trays with element size of 0.02m. Both patch and patch 2 are set to be the same as the previous designs. With this mesh control, both of skewness and aspect ratio were successfully in the acceptable, where they were found to be 0.938 and 14.12 respectively as shown if Figure 4.8 (a) and (b).

(a) (b)

Figure 4.6: (a) Edge Sizing, (b) Edge Sizing 2.

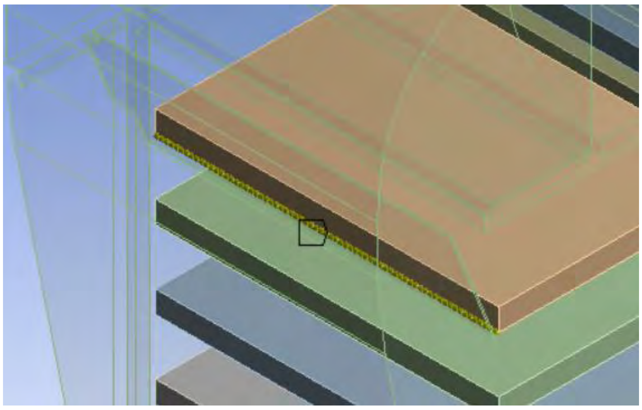

Figure 4.7: Edge Sizing 3.

Nodes	612907
Elements	3490496
Mesh Metric	Skewness
Min	2.5267e-005
Max	0.93773
Average	0.24419
Standard Deviation	0.12794

(a)

Nodes	612907
Elements	3490496
Mesh Metric	Aspect Ratio
Min	1.159
Max	14.123
Average	1.8859
Standard Deviation	0.49518

(b)

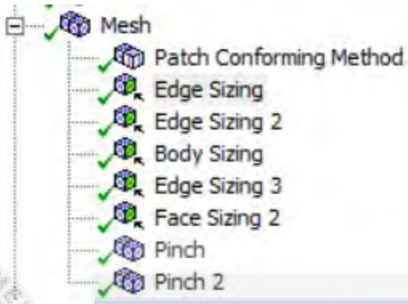

(c)

Figure 4.8: Two column-one level trays design (a) Number of nodes, elements, and the mesh metric of the skewness statistics. (b) Aspect ratio statistics (c) Mesh control tree.

4.2 SET UP

In this stage, boundary conditions, models, and materials are being selected to be applied on the design to simulate the realistic aspect. Since this simulation has been validated (Misha. S, 2013), therefore the setup of this model will be same as the validated simulation. It was very important that the residuals of a certain design's calculation to be converged. Where solution convergence is the accomplishment of a constraining behaviour in the solution of the equations, and is commonly represented by the decreasing residuals of the numerical solution. The following set up was applied to all models.

The general set up for this simulation is pressure based, absolute velocity formulated, steady in time, and gravity condition is applied as well. The energy and k-epsilon model are being used in this simulation. The material of the trays is made of Kenaf and air is used as a media in the drying system.

For the boundary condition, in inlet1 is set to have mass flow rate of 0.292 kg/s and 52 degrees Celsius, where inlet2 mass flow rate is to be half of inlet1 and the temperature is constant. The temperature of the outlet is set be 34 degrees Celsius. For the walls and roof, they are set to have a heat flux of 4 w/m2 and free steam temperature to be 32 degrees Celsius. By using these setups, the calculations were run with a number of iterations of 5000 for all designs. Figure 4.9 shows the residuals and the number of iterations for the convergence. The calculations took 424 iterations for three column-one level design to reach its convergence. Figure 4.10 shows the residuals and the number of iterations for the convergence of design's equations. The calculations took 185 iterations for up staging design to reach its convergence.

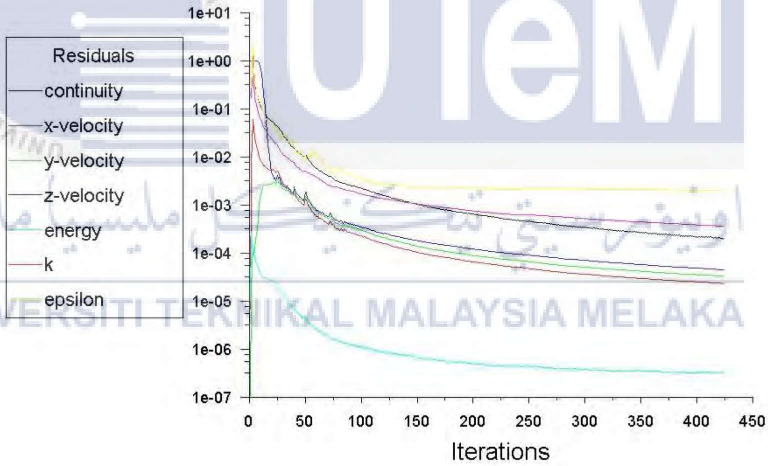

Figure 4.9: Scaled residuals of three column-one level design.

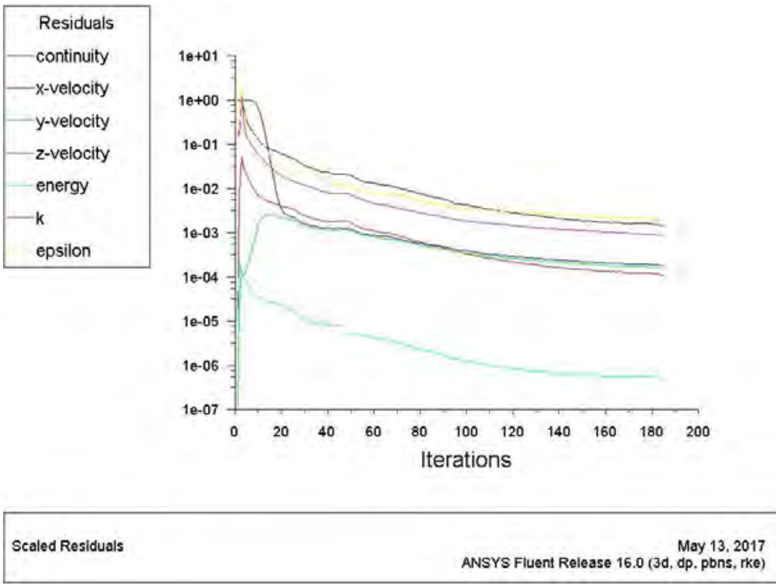

Figure 4.10: Scaled residuals of up staging design.

In the case of two column-one level, after running the calculations the scaled residuals of all seven equations were fluctuating at certain level. Where all the equations had reached their level of convergence, except the continuity equation the was almost constant at certain values. That issue could cause to inaccurate results. The reason behind this problem could be the mesh or the location of the outlet of the flow. Due to the unforeseen time constrain in this semester it was advisable to not make any further improvements to the mesh or geometry of the design.

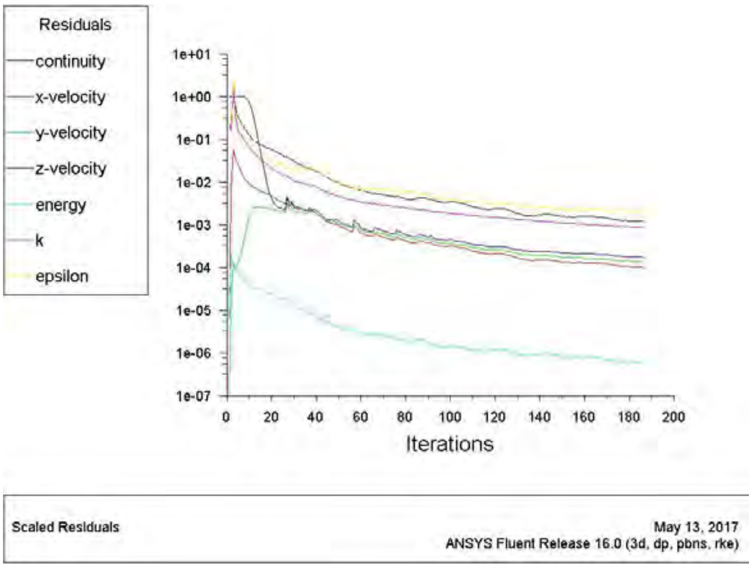

Figure 4.11: Scaled residuals of three column-tilted design.

However, the calculations for three column-tilted design were successfully reached their convergence for all equations. Figure 4.11 shows the scaled residuals and the number of iterations for the convergence of this design. Where the calculations took 186 iterations for up staging design to reach its convergence.

4.3 MESH ADAPTION

Mesh adaption is the modification on the mesh in order to get even more fine mesh on a specific area, and it serves the purpose of capturing flow features as well as increase mesh resolution to improve the accuracy of the results. In this stage, all designs mesh is adapted and run through calculations, to compare them to its non-adapted calculations. The comparison was done to check the level of accuracy and reliability of the results before and after the mesh adaption.

The steps of generating mesh adaption for all designs are generally the same, where the first step was to create an adapted gradient for velocity and temperature. Also in this step, the Refine Threshold is set to be 10% percent of the max field value that was reported. Next step would be selecting the region. By keying in the coordinates of the specific region, the region adapted was created. The third step is to combine all three of these marked cells and adapt the combination. In order to create the plots that serves the comparison, it was necessary to create line surface as reference of this comparison. Table 4.1 shows the coordinates that were selected to create the line surface which is located in front of the first column.

Line	x_0	y_0	z_0	x_1	y_1	z_1
Front line	$0.384m$	$0.22m$	$2.68m$	$0.384m$	$1.7m$	$2.68m$

Table 4.1: Front line coordinates.

Since the process of creating mesh adaption were the same for all models, therefore the general results were almost identical. Figure 4.12 (a), (b), and (c) shows the marked cells of the velocity gradient of all the models. It was found that all models had the marked cells located at the inlet and outlet. Figure 4.13 (a), (b), and (c) shows the marked cells of the temperature gradient, where the marked cells were located on the surfaces of the wall of the drying chamber. Figure 4.14 (a), (b), and (c) shows the marked cells of the specific region. The region was selected to be the trays in the drying chamber. The coordinates of the selected region are shown in Table 4.2. After the cells had been marked, they were combined and adapted. Figure 4.15(a), (b), and (c) shows the combination of the marked cells. Table 4.4 (a), (b), and (c) show the changes in nodes and faces after the mesh adaption.

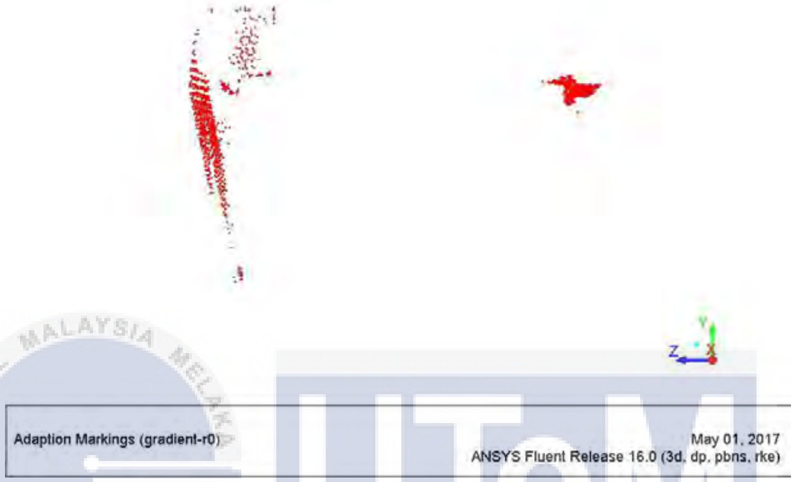

(a)

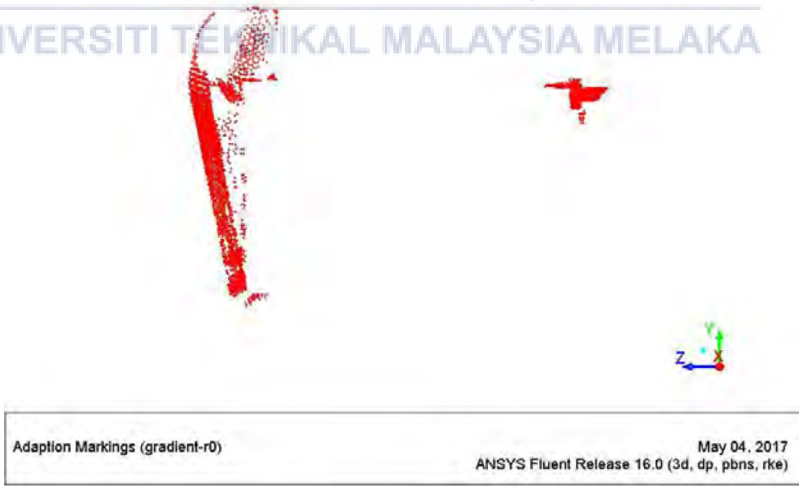

(b)

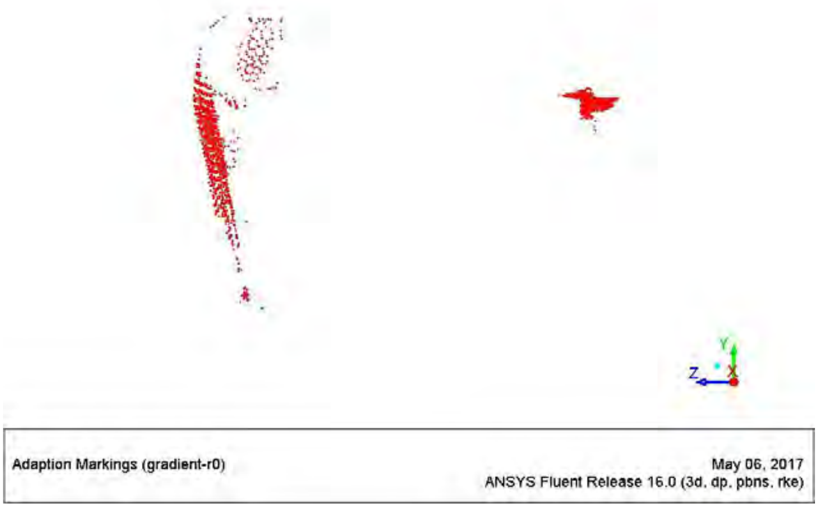

(c)

Figure 4.12: Velocity gradient marked cells (a) Three column-one level design (b) Up-staging design (c) Three column-tilted trays design

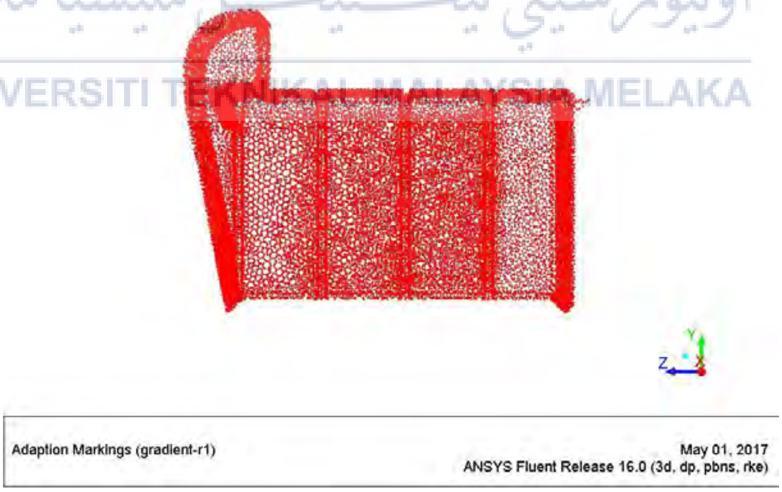

(a)

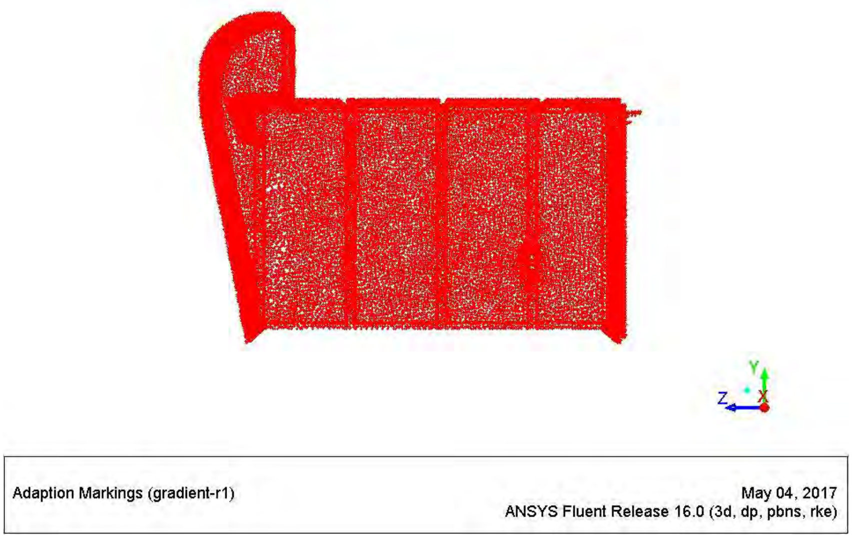

(b)

(c)

Figure 4.13: Temperature gradient marked cells (a) Three column-one level design (b) Up-staging design (c) Three column-tilted trays design.

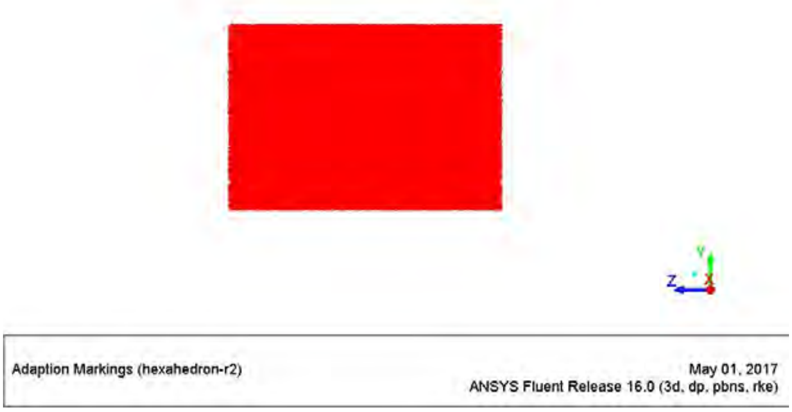
Adaption Markings (hexahedron-r2)
May 01, 2017
ANSYS Fluent Release 16.0 (3d, dp, pbns, rke)

(a)


Adaption Markings (hexahedron-r3)
May 04, 2017
ANSYS Fluent Release 16.0 (3d, dp, pbns, rke)

(b)

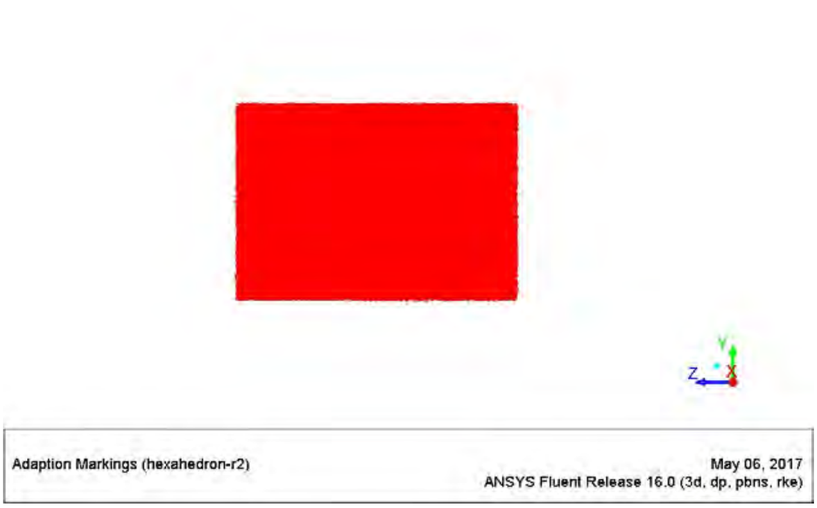

(c)

Figure 4.14: Region marked cells (a) Three column-one level design (b) Up-staging design (c) Three column-tilted trays design

	x	y	z
Min	1 m	0.15 m	0.603341 m
Max	0 m	1.53 m	2.626 m

(a)

	x	y	z
Min	1 m	0.15 m	0.603341 m
Max	0 m	1.59 m	2.626 m

(b)

	x	y	z
Min	1 m	0.15 m	0.603341 m
Max	0 m	1.5698 m	2.626 m

(c)

Table 4.2: Coordinates of the selected region (a) Three column-one level design (b) Up-staging design (c) Three column-tilted trays design.

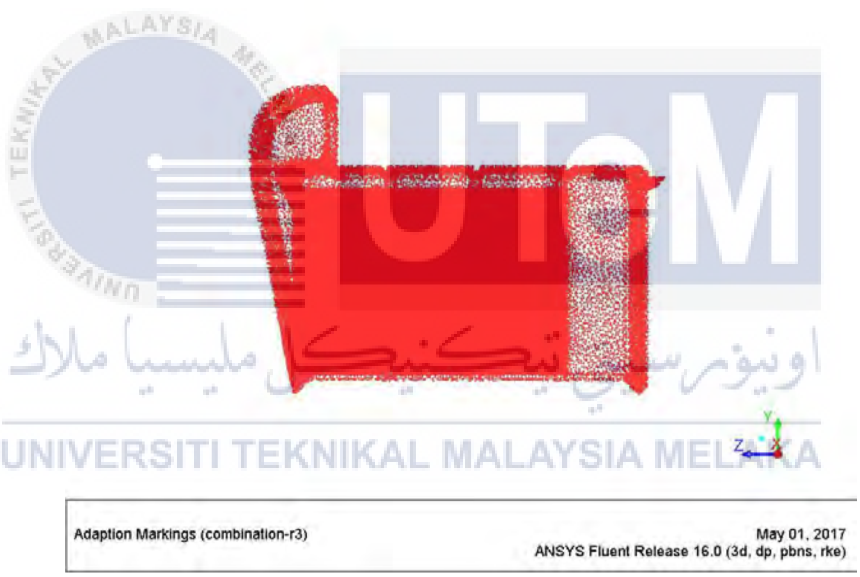

(a)

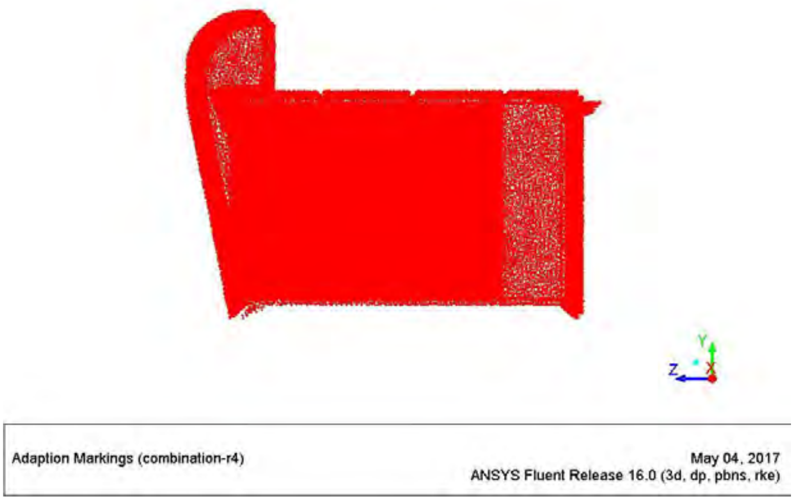

(b)

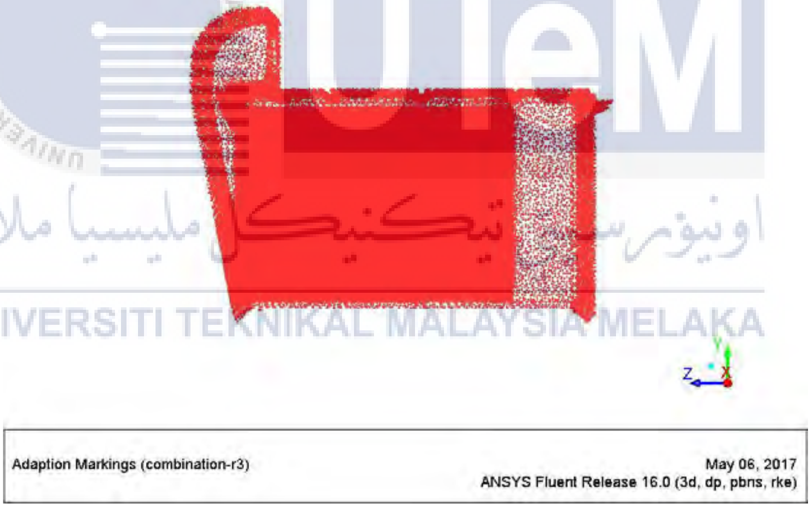

(c)

Figure 4.15: combination of the marked cells (a) Three column-one level design (b) Up-staging design (c) Three column-tilted trays design.

GRID SIZE	Original	Adapted	Change
Cells	611844	888092	276248
Faces	1234330	1842749	608419

(a)

GRID SIZE	Original	Adapted	Change
Cells	794166	4551199	3757033
Faces	1604592	9212831	7608239

(b)

GRID SIZE	Original	Adapted	Change
Cells	616875	4067315	3450440
Faces	1244476	8211692	6967216

(c)

Table 4.3: Changes in nodes and faces after the mesh adaption (a) Three column-one level design (b) Up-staging design (c) Three column-tilted trays design.

The number of iteration that ensued the mesh adaption were carried from the converged iteration. The mesh adapted three column-one level design had 57 more iteration to reach the convergence. The adapted mesh up-staging design had 55 more iteration to reach the convergence. While the mesh adapted three column-tilted trays design had 2 more iteration to reach the convergence. In order to verify the accuracy and reliability of the result, the results of the non-adapted designs with the adapted ones. If both results of the same design were over lapping in the plot or very near each other, that indicates that the results are accurate reliable. If both results of the same design weren't over lapping in the plot or very near each other, that indicates that the results aren't accurate or reliable. This problem can be solved by repeating the mesh adaption, re-running calculation, and comparing the results to check the accuracy.

These steps will have to be repeated until the plots are over lapping. As can be noticed from Figure 4.16 (a) and (b), Figure 4.17 (a) and (b), and Figure 4.18 (a) and (b) the results of velocity magnitude and static temperature are nearly over lapping of all designs. Where the red dots represent the results of the design without mesh adaption, and the black dots represent the results of the design with mesh adaption.

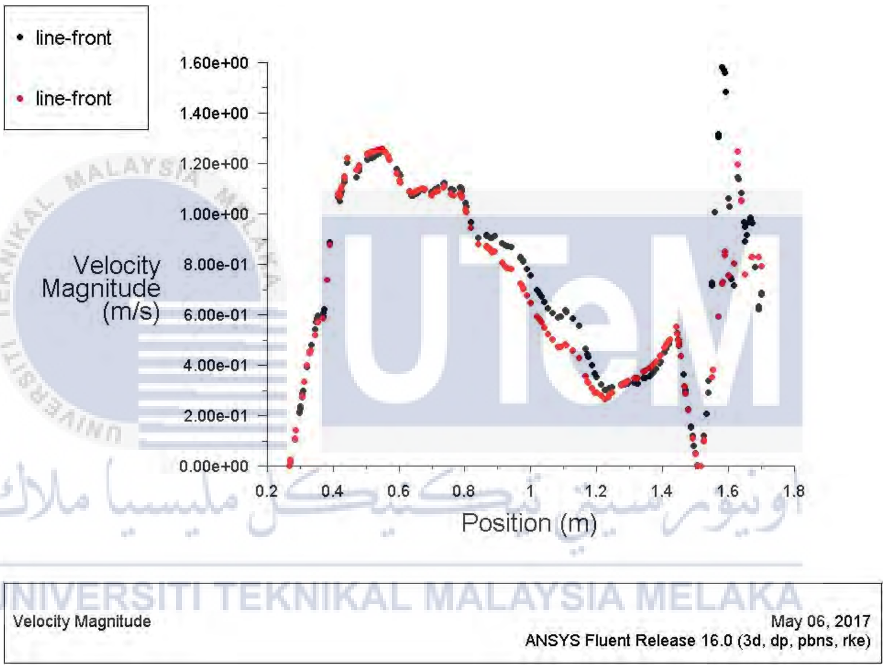

(a)

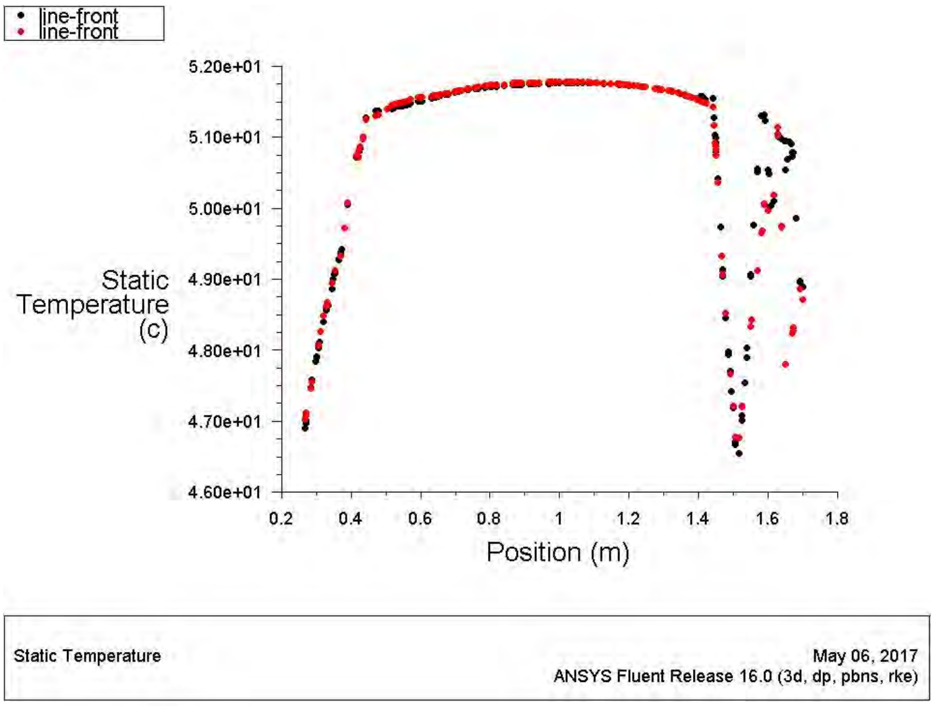

(b)

Figure 4.16: Three column-one level design (a)velocity magnitude (b) Static temperature.

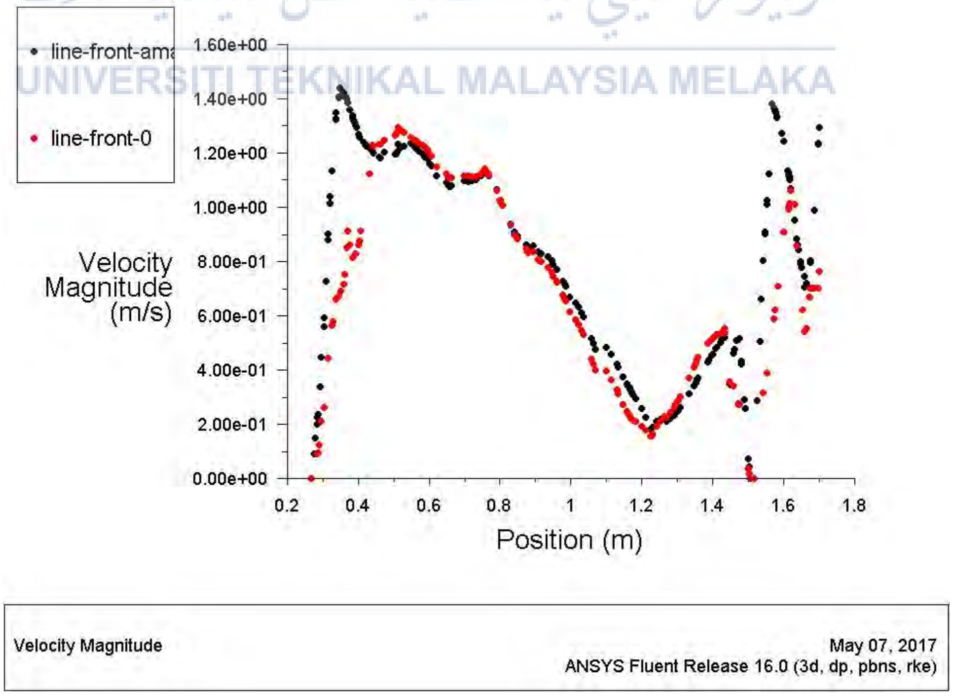

(a)

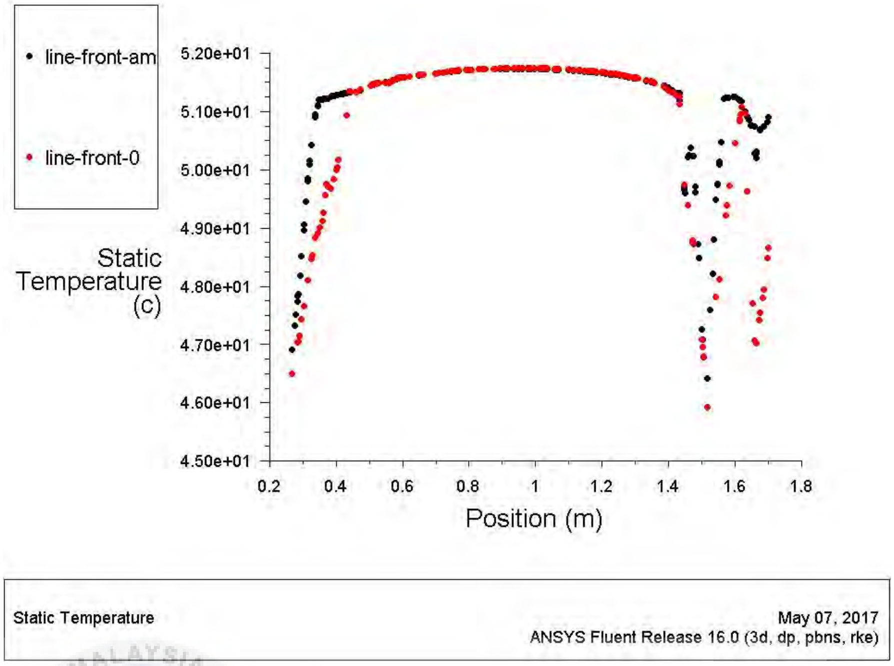

(b)

Figure 4.17: Up-staging design (a)velocity magnitude (b) Static temperature.

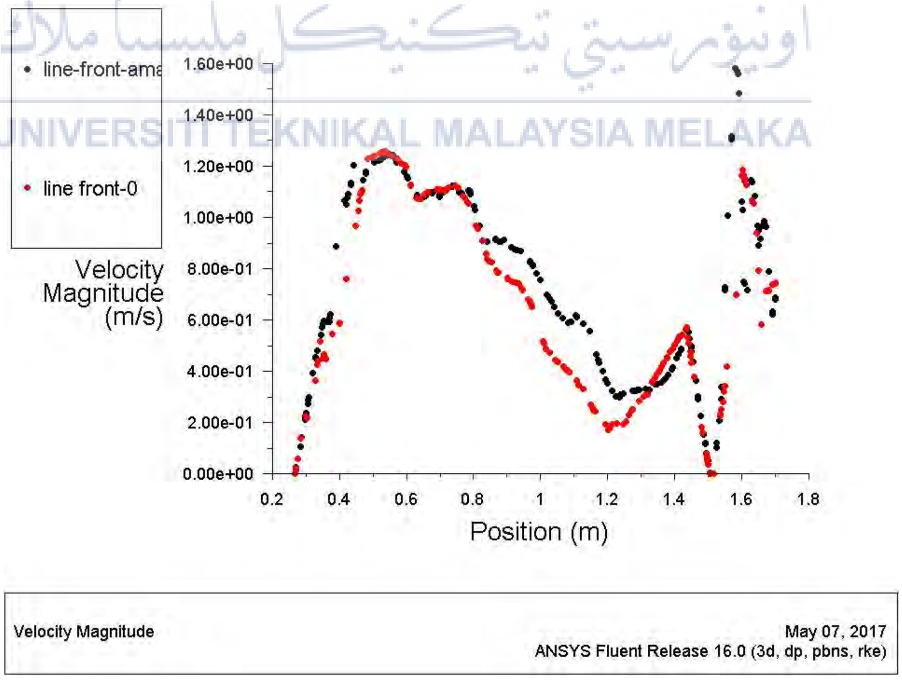

(a)

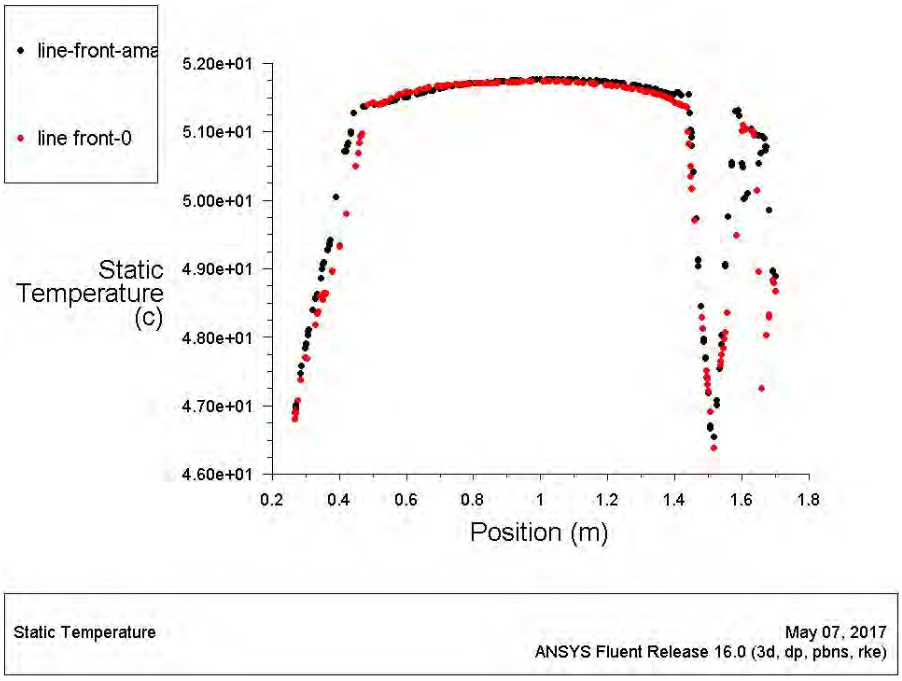

(b)

Figure 4.18: Three column-tilted trays design (a)velocity magnitude (b) Static temperature.

4.4 RESULTS

4.4.1 Three column-one level design

Average velocity, air flow distribution, and the temperature of the drying chamber are the main contributors in determining the drying rate. As result, Studying the results of each help in understanding the problem and improving the simulation to meet the validated simulation. Figure 4.19 shows the temperature distribution in the drying chamber. First column and second have a higher temperature than the third column.

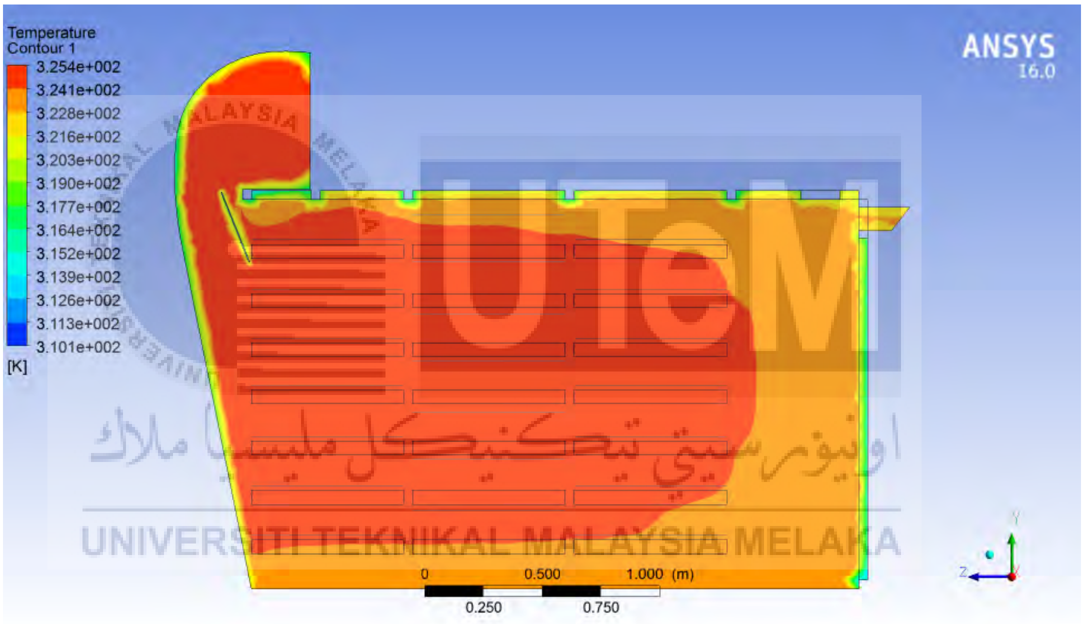

Figure 4.19: Temperature contour of three column-one level design.

Figure 4.20 shows the air flow distribution in the drying chamber. the air flow is distributed almost equally at every row except the top row. Due to the existence of the baffle, the air is separated at the front face creating a turbulent flow. This arrangement of the trays allows the air to flow almost in a straight line on top of the trays.

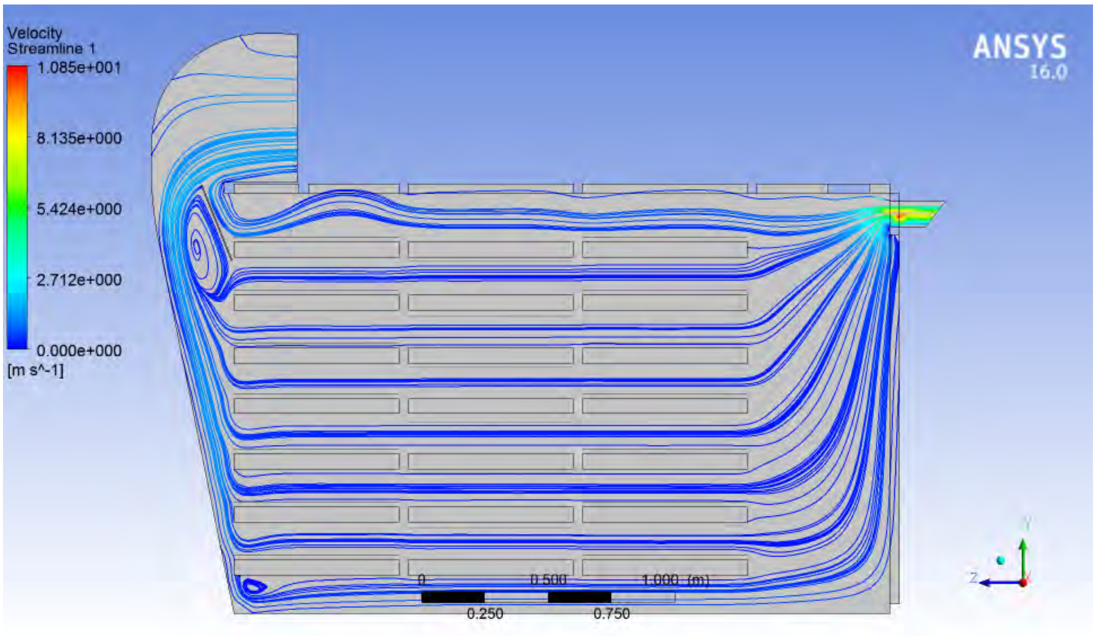

Figure 4.20: Air streamlines of three column-one level design.

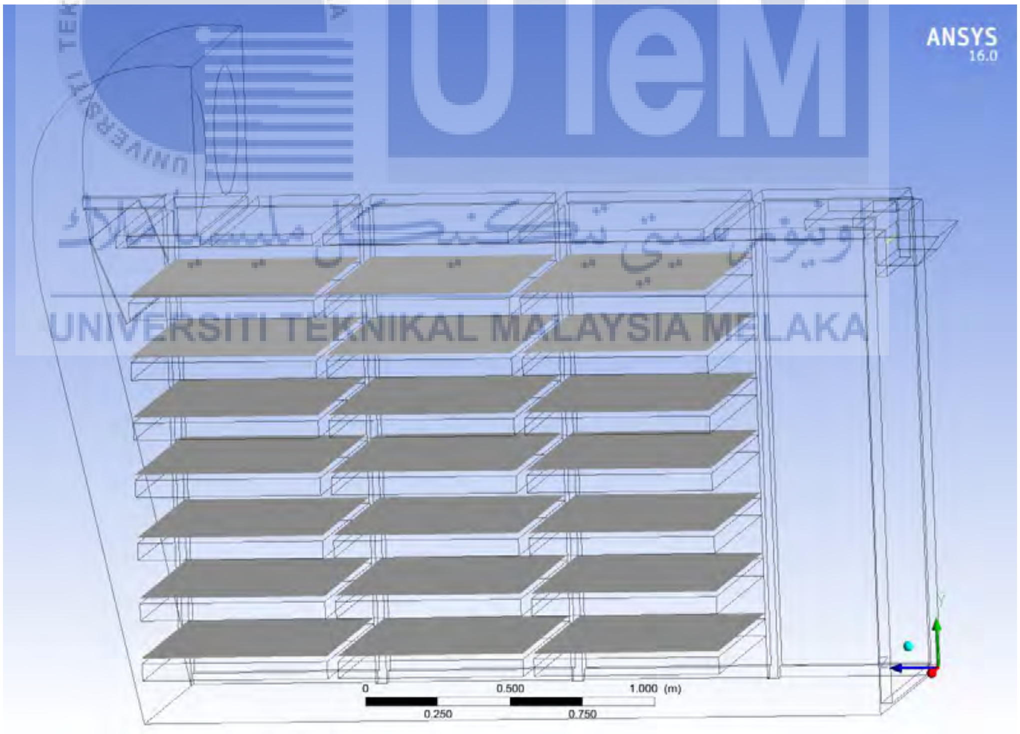

Figure 4.21: Average velocity plane.

By creating a plane on 2 cm on top of each tray, the average velocity of each tray can be measured as shown in Figure 4.21. Table 4.4 and Figure 4.22 show each tray with its average velocity. It was found that top front tray 1 has the highest velocity and tray

15 has the second highest average velocity although it is positioned the last column. This is due to the location of the outlet. The outlet and the position of tray 15 are close, therefore it acts as point were some of the flow of the other trays passes tray 15. Which it increases the average velocity of tray 15.

Tray No.	Average velovcity (m/s)
1	0.4270
2	0.1883
3	0.2067
4	0.1837
5	0.2397
6	0.2259
7	0.2580
8	0.2168
9	0.1705
10	0.1605
11	0.1412
12	0.1882
13	0.1665
14	0.1591
15	0.2567
16	0.1232
17	0.1479
18	0.1299
19	0.1705
20	0.1461
21	0.1285
max	0.4270
min	0.1232
ave	0.1921
gap	0.3038

Table 4.4: Trays average velocity of three column-one level design.

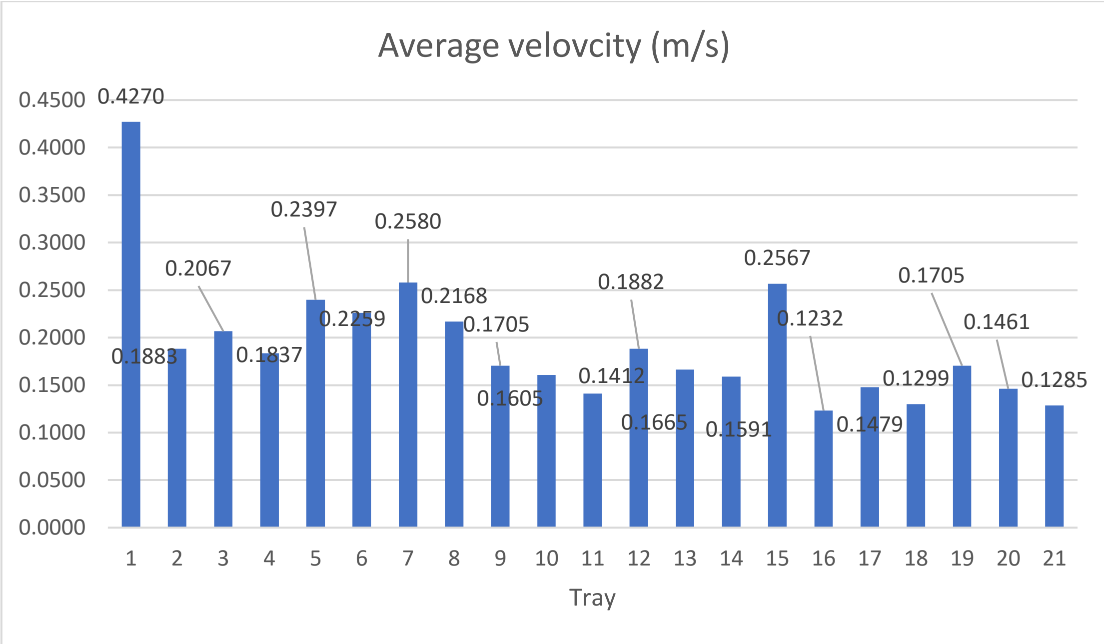

Figure 4.22: Average velocity of three column-one level design.

Tray 1 being the highest average velocity and tray 16 being the lowest average velocity, the gap is 0.3038 m/s. The gap represents the uniformity of the air flow distribution in the drying chamber. Where a lower gap in the average velocity leads to more uniform air flow distribution. The average velocity of the whole drying chamber is being 0.1921 m/s. A high average velocity of the drying chamber leads to a lesser drying time.

4.4.2 Up-staging design

In up-staging design, Figure 4.23 shows the velocity streamlines. The air flows following the trays positions. While Figure 4.24 shows the temperature after mesh adaption. The temperature of the first column is higher than the second one, while the second column has a higher temperature than the third column. Also, the temperature at tray 3, 4, 5, 10, 11, and 12 are the highest comparing to the rest of the trays. It can be noticed that tray 15 has the second highest average velocity after tray 1 as shown Table 4.5 and Figure 4.25. This is due to the position of the tray, which it creates a small area between the roof and the surface of the tray. Which it increases the average velocity of tray 15. Tray 1 being the highest average velocity and tray 21 being the lowest average velocity, the gap is 0.2264 m/s. The average velocity of the whole drying chamber is being 0.1990 m/s.

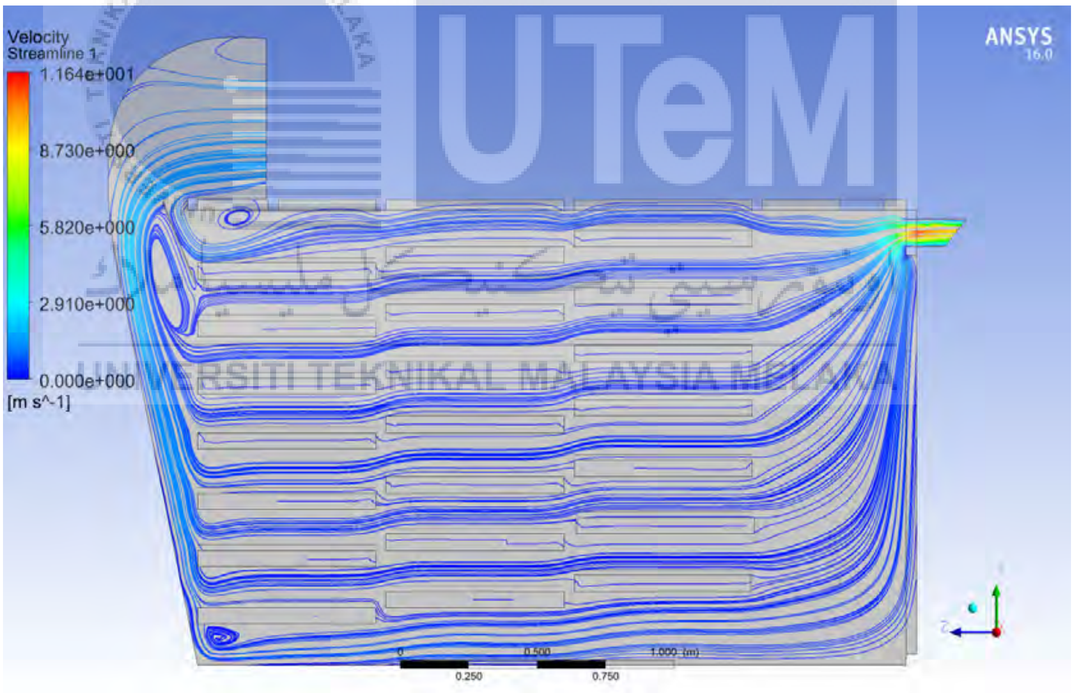

Figure 4.23: Air streamlines of up-staging design.

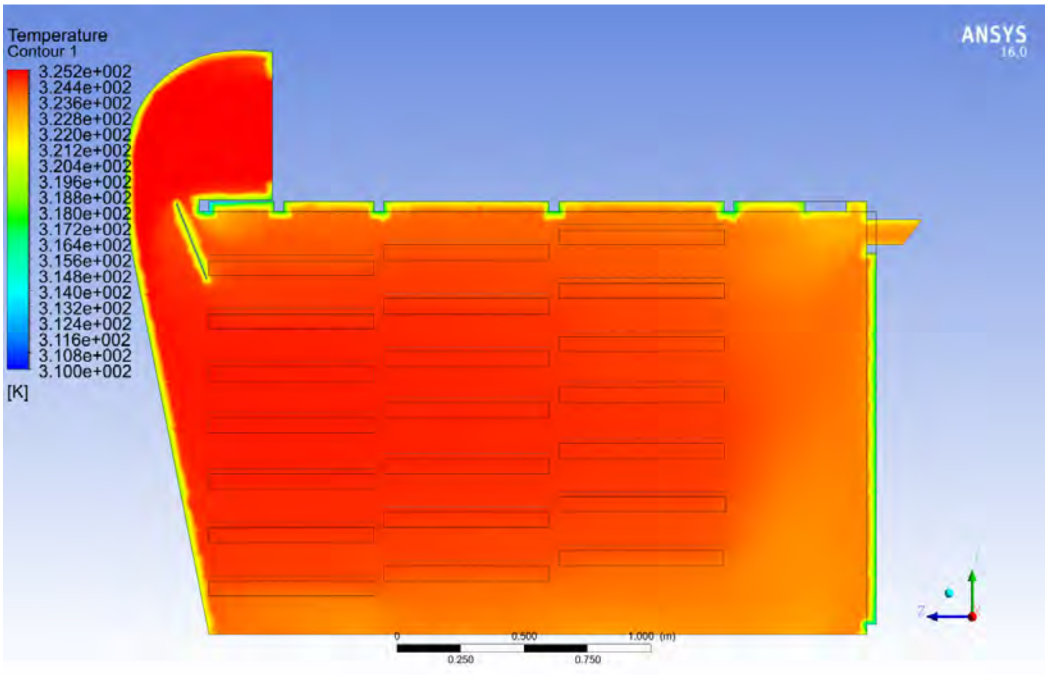

Figure 4.24: Temperature contour of up-staging design.

Tray No.	Average velovcity (m/s)
1	0.3418
2	0.1637
3	0.2019
4	0.1893
5	0.2328
6	0.2254
7	0.2429
8	0.2216
9	0.1730
10	0.1772
11	0.1556
12	0.1858
13	0.1687
14	0.1459
15	0.3186
16	0.2217
17	0.2029
18	0.1631
19	0.1823
20	0.1495
21	0.1154
max	0.3418
min	0.1154
ave	0.1154
gap	0.1990

Table 4.5: Trays average velocity of up-staging design.

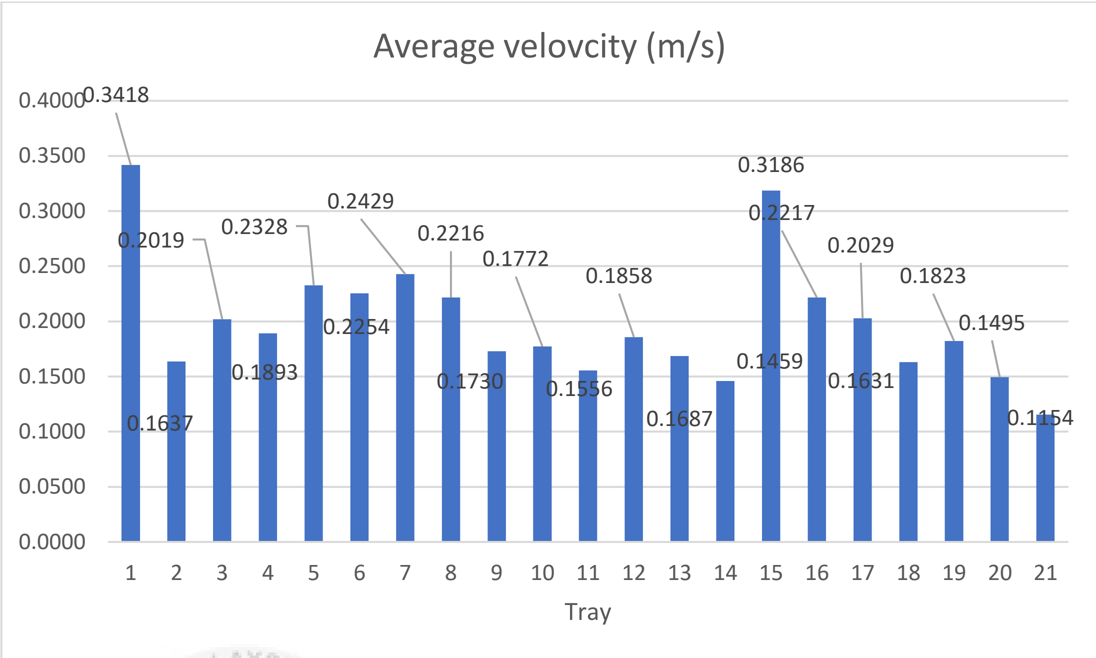

Figure 4.25: Average velocity of up-staging design.

4.4.3 Three column-tilted trays design

Much like, Figure 4.26 shows the velocity streamlines. The air flows following the trays positions. While Figure 4.27 shows the temperature after mesh adaption. The temperature of the first column is higher than the second one, while the second column has a higher temperature than the third column. Also, the temperature at tray 3, 4, 5, 10, 11, 12, 17, 18, and 19 are the highest comparing to the rest of the trays. It can be noticed that tray 15 has the second highest average velocity after tray 1 as shown Table 4.6 and Figure 4.28. This is due to the tilt of the tray, which it creates a small area between the roof and the surface of the tray. In addition, the tilt of the second and third column help guiding the flow. Which it increases the average velocity of tray 15. Tray 1 being the highest average velocity and tray 10 being the lowest average velocity, the gap is 0.25799 m/s. The average velocity of the whole drying chamber is being 0.1968 m/s.

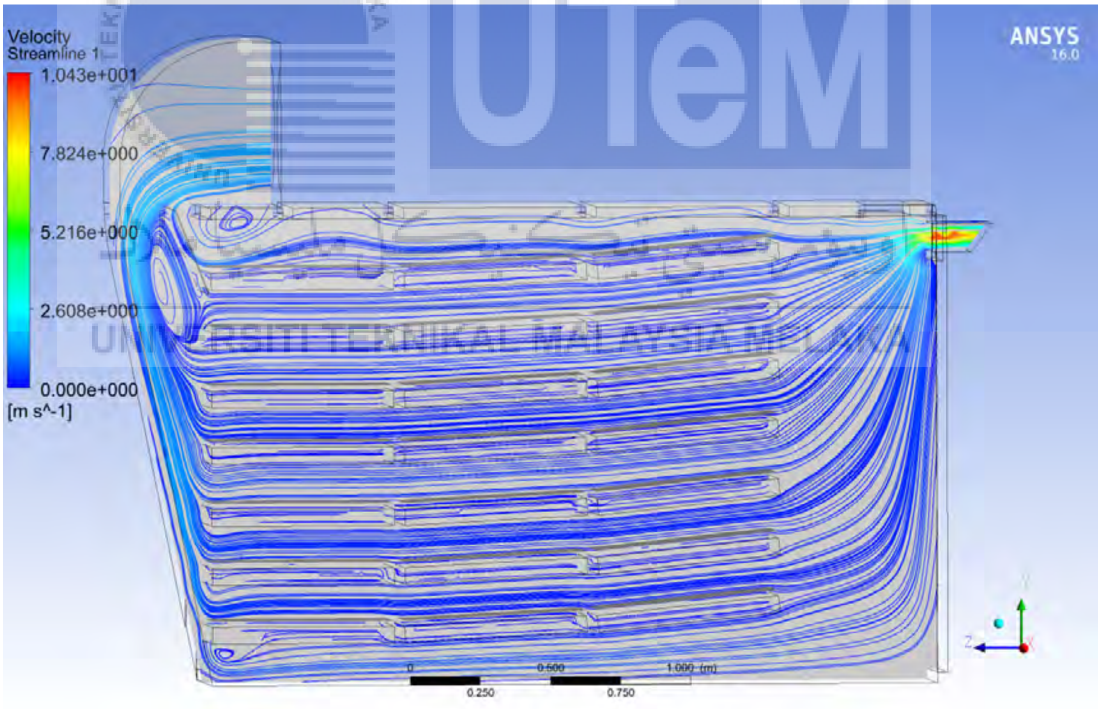

Figure 4.26: Air streamlines of three column-tilted trays design.

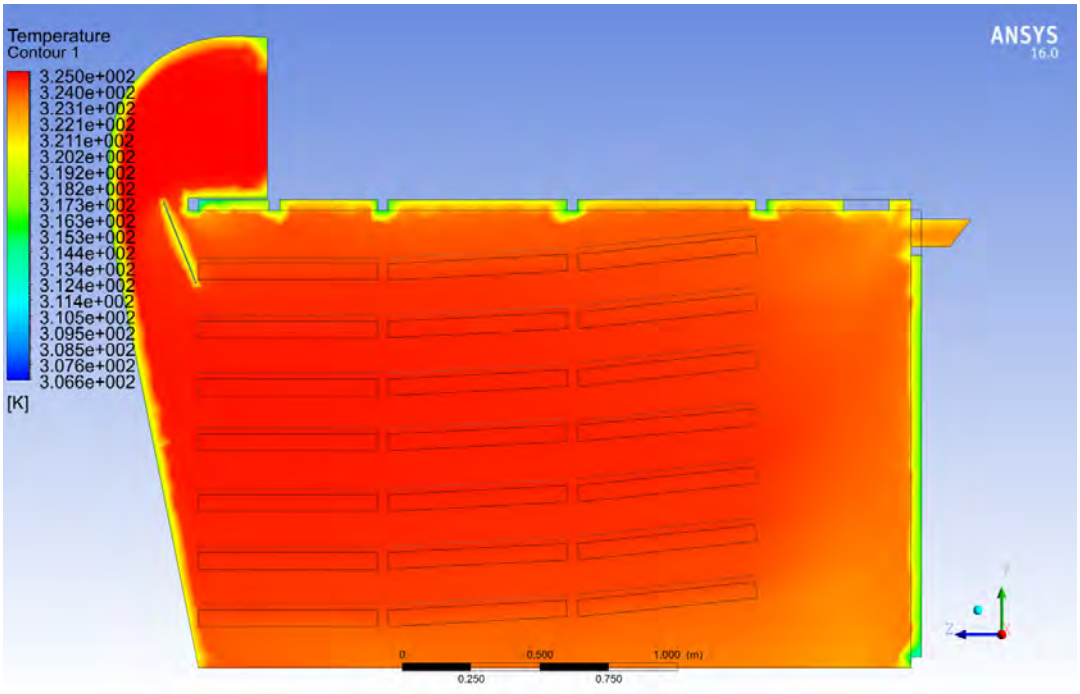

Figure 4.27: Temperature contour of three column-tilted trays design.

Tray No.	Average velovcity (m/s)
1	0.35490
2	0.18770
3	0.20480
4	0.19790
5	0.24490
6	0.23620
7	0.24080
8	0.19480
9	0.14730
10	0.09691
11	0.15000
12	0.18190
13	0.16790
14	0.13810
15	0.32030
16	0.20710
17	0.19750
18	0.18830
19	0.18980
20	0.16730
21	0.11780
max	0.3549
min	0.09691
ave	0.196772
gap	0.25799

Table 4.6: Trays average velocity of three column-tilted trays design.

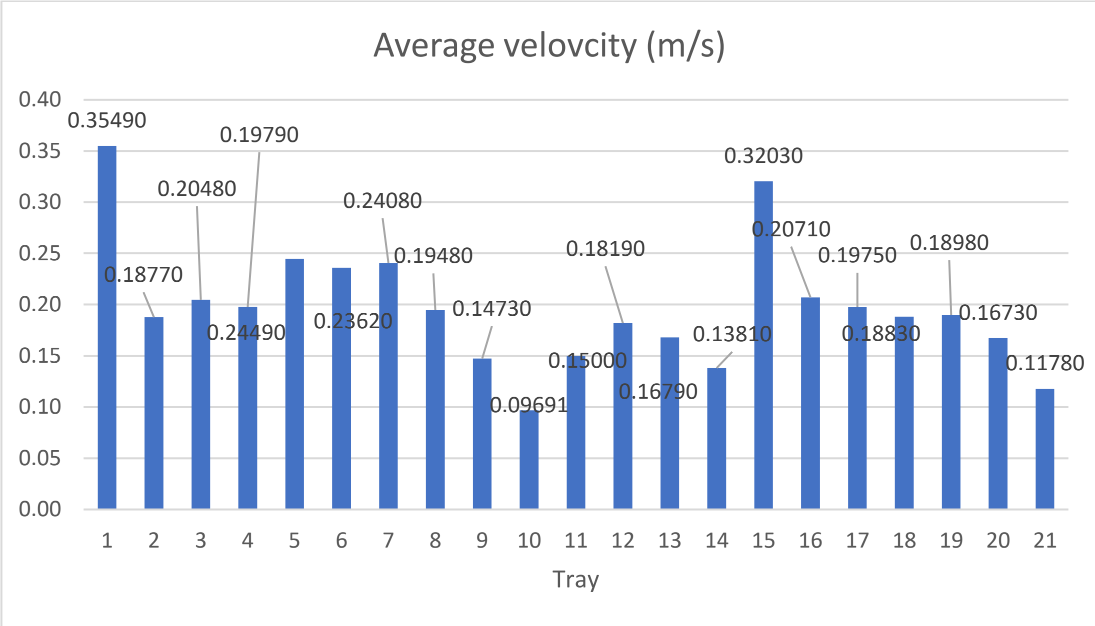

Figure 4.28: Average velocity of three column-tilted trays design.

4.4.4 Summary

Design	Three column-one level	Up-staging	Three column-tilted trays
Average velocity(m/s)	0.1921	0.1990	0.1968
Maximum average velocity (m/s)	0.4270	0.3418	0.3549
Minimum average velocity(m/s)	0.1232	0.1154	0.0969
Gap (m/s)	0.3038	0.2264	0.2580

Table 4.7: Summary of designs and results

Table 4.7 shows the summary of designs and their results. This comparison is done to determine the most suitable design that meets the main purpose of this project. It was found that up-staging design has the highest average velocity throughout the drying chamber as well as the lowest gap between the maximum and the minimum average velocity of the trays. Based on these results, the up-staging design has the highest air flow distribution on the trays comparing to the other suggested designs.

CHAPTER 5

CONCLUSION AND RECOMMENDATION

5.1 Conclusion

In conclusion, only three designs were successfully simulated. Two column-one level trays design was not simulated. This is due to the convergence of its equations, where the calculations of its equations were not converged. The results of the simulated designs show the average velocity of each tray, the average velocity of the drying chamber, and the gap between the maximum and minimum average velocity of the trays. Where the gap of three column-one level design is 0.3038 m/s, up-staging design is 0.2264 m/s, and three column-tilted trays design 0.25799 m/s. The average velocity of three column-one level design is 0.1921 m/s, up-staging design is 0.1990 m/s, and three column-tilted trays design 0.1968 m/s. A high average velocity and a low gap value determine the most uniform air flow distribution. Up-staging design has the lowest gap and the highest average velocity values among the other two designs. Hence, the up-staging design has the best air flow distribution.

5.2 Recommendation

Based on the suggested designs and its results, it was clear that up-staging had the best air flow distribution among all designs. It noticed that tilted tray design had a better air distribution than same level-one column tray design. Therefore, it is recommended that a further improvement on tilted tray design. Where improving this design could lead to a better air flow distribution in the drying chamber. Since two column-one level trays design could not get through its calculation, it is recommended that an accurate and better quality of mesh need to be created in order study the potential of this design.

CHAPTER 6

References

1. Ahmad Fudholi, K. S. (2014). Performance analysis of solar drying system for red chili. Solar Energy 99, 47-54.

2. ANSYS, I. (February 14, 2011). Solving a Conjugate Heat Transfer Problem using ANSYS FLUENT. ANSYS, Inc.`

3. Arnab Ganguly, A. A. (2012). Modeling and measurements of water–vapor flow and icing at low pressures with application to pharmaceutical freeze-drying. International Journal of Heat and Mass Transfer 55 , 5503–5513.

4. Chao Jia, L. W. (2016). Effect of swing temperature and alternating airflow on drying uniformity. Applied Thermal Engineering 106, 774-783.

5. Chr. Lamnatou, E. P. (2010). Finite-volume modelling of heat and mass transfer during convective drying of porous bodies - Non conjugate and conjugate formulations involving the aerodynamic effects. Renewable Energy Vol.35, 1391-1402.

6. Defraeye, T. (2017). When to stop drying fruit: Insights from hygrothermal modelling. Applied Thermal Engineering 110, 1128-1136.

7. Ghasemkhani .H, K. .. (2016). Improving exergetic performance parameters of a rotating-tray. Applied Thermal Engineering 94, 13–23.

8. M.M. Morad, M. E.-S.-M. ((2017) 9). Thermal analysis and performance evaluation of a solar tunnel. Renewable Energy 101, 992-1004.

9. Misha .S, M. .. (2012). Review of solid/liquid desiccant in the drying applications. Renewable and Sustainable Energy Reviews 16, 4686–4707.

10. Misha .S, M. .. (2013). Comparison of CFD Simulation on Tray Dryer System. Latest Trends in Renewable Energy and Environmental Informatics, -.

11. Misha .S, S. M. (2013). Review on the Application of a Tray Dryer System for Agricultural Products. World Applied Sciences Journal 22(3), 424-433.

12. Misha, S. B. (2015). PEMBANGUNAN SISTEM PENGERINGAN TERBANTU SURIA DENGAN PENYAHLEMBAPAN PEPEJAL UNTUK PRODUK PERTANIAN. thesis, -.

13. N. A. Vlachos, D. K. (2002). DESIGN AND TESTING OF A NEW SOLAR TRAY DRYER. DRYING TECHNOLOGY, 20(5), 1239–1267.

14. Nabnean .S, J. .. (2016). Experimental performance of a new design of solar dryer for drying. Renewable Energy 94, 147-156.

15. SAS IP, I. (n.d.). sharcnet. Retrieved from www.sharcnet.ca: https://www.sharcnet.ca/Software/Ansys/17.0/en-us/help/flu_ug/flu_ug_mesh_quality.html

16. Suhaimi Misha, S. M. (2013). The CFD Simulation of Tray Dryer Design For Kenaf Core Drying. Applied Mechanics and Materials Vol. 393, 717-722.

17. Tadahmun A. Yassen, H. H.-K. (2016). Experimental investigation and evaluation of hybrid solar/thermal dryer. Solar Energy 134, 284-293.

18. Team, L. C. (2013 , Jul 1). computational fluid dynamics. Retrieved from LEAP's Computational Fluid Dynamics (CFD): http://www.computationalfluiddynamics.com.au/tips-tricks-cfd-estimate-first-cell-height/

19. Wikipedia. (2016, 9 3). Solar dryer. Retrieved from Wikipedia: https://en.wikipedia.org/wiki/Solar_dryer

20. Xiaolong Lei, Y. L. (2016). Simulation of seed motion in seed feeding device with DEM-CFD. Computers and Electronics in Agriculture 131, 29–39.

21. Finzer, J. R. D., Menezes, E. A., & Limaverde, J. R. (1997). Drying coffee beans in vibrated trays dryer. Drying technology, 15(6-8), 1983-1994.

22. Amanlou, Y., & Zomorodian, A. (2010). Applying CFD for designing a new fruit cabinet dryer. Journal of food engineering, 101(1), 8-15.

23. Mathioulakis, E., Karathanos, V. T., & Belessiotis, V. G. (1998). Simulation of air movement in a dryer by computational fluid dynamics: application for the drying of fruits. Journal of Food Engineering, 36(2), 183-200.

24. Hancioglu, E., Hepbasli, A., Icier, F., Erbay, Z., & Colak, N. (2010). Performance investigation of the drying of parsley in a tray dryer system. International Journal of Exergy, 7(2), 193-210.

25. Colak, N., & Hepbasli, A. (2007). Performance analysis of drying of green olive in a tray dryer. Journal of Food Engineering, 80(4), 1188-1193.